The Effect of Graphene Oxide and its Oxidized Debris on the Cure Chemistry and Interphase Structure of Epoxy Nanocomposites

Dilini G.D. Galpaya, Joseph F.S. Fernando, Llew Rintoul, Nunzio Motta, Eric R. Waclawik, Cheng Yan*, Graeme A. George*

School of Chemistry, Physics and Mechanical Engineering, Faculty of Science and Engineering, Queensland University of Technology, GPO Box 2434, Brisbane, 4001, Australia

ABSTRACT

The influence of graphene oxide (GO) and its surface oxidized debris (OD) on the cure chemistry of an amine cured epoxy resin has been investigated by Fourier Transform Infrared Emission Spectroscopy (FT-IES) and Differential Scanning Calorimetry (DSC). Spectral analysis of IR radiation emitted at the cure temperature from thin films of diglycidyl ether of bisphenol A epoxy resin (DGEBA) and 4,4'-diaminodiphenylmethane (DDM) curing agent with and without GO allowed the cure kinetics of the interphase between the bulk resin and GO to be monitored in real time, by measuring both the consumption of primary (1°) amine and epoxy groups, formation of ether groups as well as computing the profiles for formation of secondary (2°) and tertiary (3°) amines. OD was isolated from as-produced GO (aGO) by a simple autoclave method to give OD-free autoclaved GO (acGO). It has been found that the presence of OD on the GO prevents active sites on GO surfaces fully catalysing and participating in the reaction of DGEBA with DDM, which results in slower reaction and a lower crosslink density of the three-dimensional networks in the aGO-resin interphase compared to the acGO-resin interphase. We also determined that OD itself promoted DGEBA homopolymerization. A DSC study further confirmed that the aGO nanocomposite exhibited lower T_g while acGO nanocomposite showed higher T_g compared to neat resin because of the difference in crosslink densities of the matrix around the different GOs.

KEY WORDS: Epoxy resin, Graphene oxide, Oxidative debris, Cure kinetics, Interphase, Nanocomposites, XPS, Infrared emission.

GRAPHICAL ABSTRACT

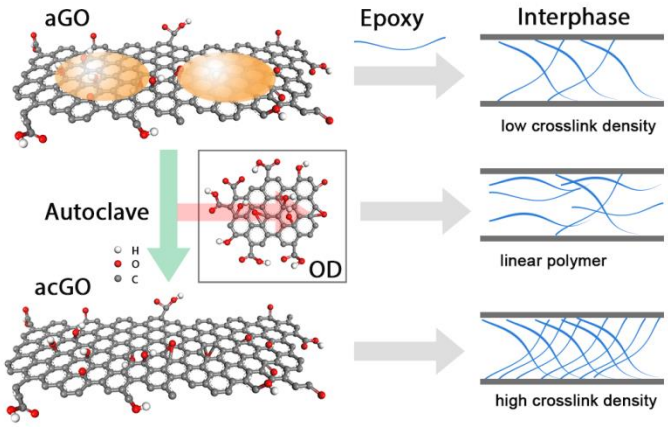

1. INTRODUCTION

Graphene oxide (GO) is a graphene derivative containing covalently attached oxygen-containing surface groups such as hydroxyl, carbonyl, carboxyl and epoxy groups. In general, it is accepted that hydroxyl and epoxy groups are bonded to the surface of graphene sheets and carboxyl groups are bound to the edges of the basal planes [1]. These functional groups can facilitate better exfoliation and dispersion in solvents and further surface functionalization [1]. Importantly, GO has an ideal surface for interacting with polymer matrices and several polymer nanocomposites with significantly improved mechanical properties have been developed [2-6]. However, it has been recently reported that as-produced GO (aGO) is a mixture, containing lightly oxidized graphene sheets and heavily oxidised low molecular weight material. This oxidised low molecular weight material, called oxidative debris (OD) resembles the complex aromatic fulvic acid that is strongly bonded to aGO surface but can be removed by washing with alkaline solutions [7]. The majority of the oxygen-containing groups found in bulk aGO are actually in OD and it is considered responsible for the observed excellent suspension in aqueous solutions as well as the fluorescence of graphene oxide [7,8]. Further, some studies reported that OD is accountable for some inherent properties of bulk GO such as electroactivity [9].

Epoxy resins are thermosetting materials possessing high stiffness, dimensional stability and chemical resistance [10]. Understanding the curing behaviour of epoxy systems is essential because the thermal and mechanical properties of the epoxy composites depends on the formation of the cross-linked molecular network in the system and the structure of the interphase

region between the continuous phase (resin) and the discontinuous phase (reinforcement). The interphase region plays a critical role in determining those properties of the composites that depend on the interfacial load transfer between resin and nanofiller. It has been shown that the dimensions of the interphase in carbon-fiber epoxy composites is 118 nm [11] so that a simple calculation shows that if the GO is fully exfoliated with a (hypothetical) surface area of 2630 m^2/g, 100% of the resin is potentially in the GO interphase region at loadings as low as 0.5wt%. Mc Allister et al.[12] in their detailed study of the expansion and exfoliation of graphite oxide to produce single-sheet GO have noted that the real surface area reduces to values of $1850 m^2/g$ when suspended in solution (determined by methylene blue adsorption) and 600-900 m^2/g in the solid state due to aggregation (as measured by the BET isotherm). These values will be even further reduced if the GO is only partially exfoliated since it has been noted for expanded graphite oxide the surface area is $<100 m^2/g$. In an epoxy resin-GO nanocomposite the effective interphase volume will depend on the method of sample preparation since exfoliation is a pre-cursor to interpenetration of the GO by the resin-hardener mix. Solution preparation involving ultrasonication [13,14] is the simplest way to achieve this. A feature of these epoxy-GO nanocomposites is that very low loadings only are required to achieve significant changes in properties, including fracture toughness[6,15-19] which implies that the structure of the interphase may be responsible for these changes. Putz et al.[20] have noted that the high surface area means that the interphase may percolate the entire volume of the nanocomposite, so dominating the usual bulk properties such as glass transition temperature (T_g).

The final properties of the cured bulk resin are also determined by the chemical structure of both the resin and the curing agent. Epoxy resins contain at least two terminal epoxide groups which can be cured by various types of curing agents such as diamines, anhydrides or isocyanates [21]. Amine curing process of epoxy generally involves three major reactions ie; 1° amine-epoxy, 2° amine-epoxy and hydroxyl-epoxy addition reactions as schematically shown in Fig. 1 [22,23].

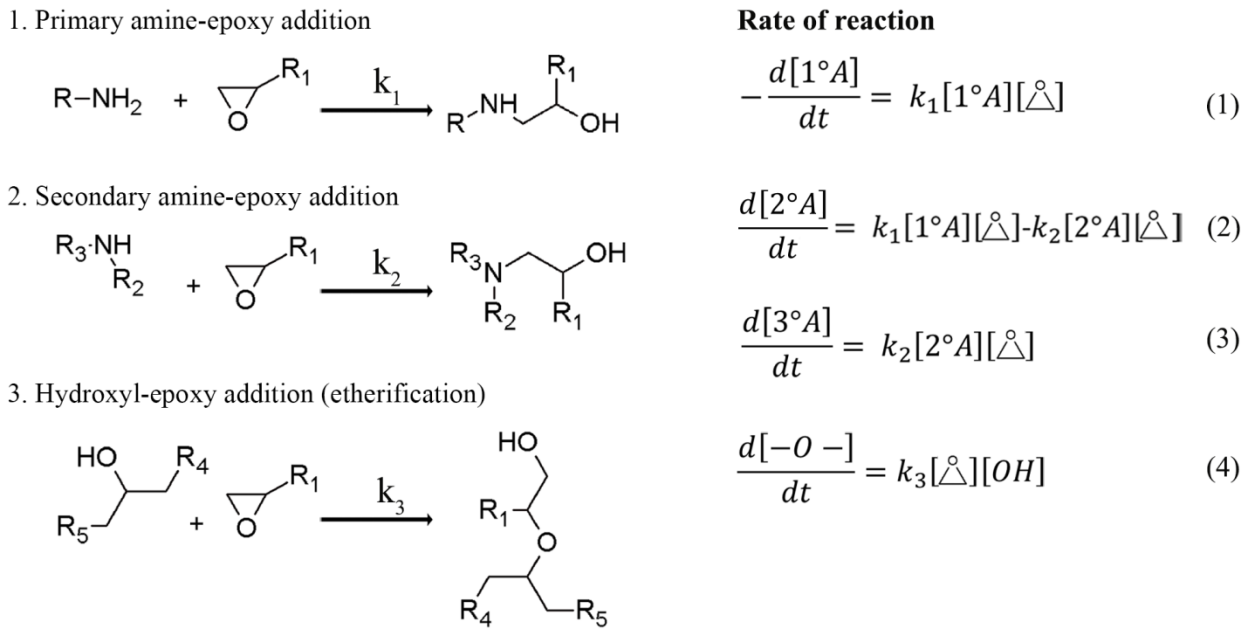

$$-\frac{d[1°A]}{dt} = k_1[1°A][\triangle] \quad (1)$$

$$\frac{d[2°A]}{dt} = k_1[1°A][\triangle] - k_2[2°A][\triangle] \quad (2)$$

$$\frac{d[3°A]}{dt} = k_2[2°A][\triangle] \quad (3)$$

$$\frac{d[-O-]}{dt} = k_3[\triangle][OH] \quad (4)$$

Fig. 1. Schematic representation of three major reactions during the amine curing of epoxy resin and empirical equations for the rate of these reactions. Note that there are two epoxide and two 1° amine groups per molecule in the DGEBA-DDM system (see Fig. 2).

The amine curing processes and reaction mechanisms of several epoxy resin systems have been widely investigated by means of differential scanning calorimetry (DSC)[10,15,24], dynamic mechanical analysis (DMA)[25] raman spectroscopy [26,27], near-infrared (NIR) spectroscopy [28], infrared emission spectroscopy (IES)[22], etc. DSC is the most widely used of these techniques due to its simplicity but it cannot provide explicit information on the chemical reactions during cure [29,30]. Analysis provides information including cure enthalpy (ΔH_{cure}), glass transition temperature (T_g), reaction exotherm (onset temperature: T_{onset}, peak temperature: T_p) and (with some assumptions) activation energy (E_a). Several research studies reported that curing reaction in epoxy matrix can be influenced by the addition of filler materials. It has been noticed that metal oxides such as zinc, aluminium and iron oxides exhibit a catalytic effect on the epoxy curing consistent with adsorption of curing agent on to the metal particle surfaces [31,32]. Moreover, interfacial effect of nanoparticles is generally higher than with micron-sized filler particles due to the much higher surface area of nanoparticles. The functional groups on the surface of GO are able to both react with the components of the epoxy resin and potentially catalyse the cure reactions. XPS and IR spectroscopy have identified oxirane, carboxylic acid and alcohol groups on GO surface [1].

Table 1

Comparison of previously reported work on effect of graphene/GO on amine-epoxy curing

Graphene derivative	Technique	Findings	Reference
GO	Non-isothermal DSC (Kissinger-Friedman analysis)	• Retardation effect	Ryu et al.[10]
GO-amine modified		• Acceleration effect • Neutralization of NH_2 by COOH-GO	
GO	DSC (ΔH, T_p, T_{onset})	• Acceleration effect • Catalytic effect on epoxy ring opening reaction by 'O' groups on GO	Bortz et al.[15]
GO	Non-isothermal DSC	• Acceleration effect	Qui et al.[33]
Graphene/GO	DSC (T_g)	• Catalytic effect on both 1° and 2° amine- epoxy reactions	Mauro et al.[34]
Graphene	DSC (ΔH, T_p)	• Retardation effect • Steric hindrance	Teng et al.[35]
Graphene	DSC (T_g)	• Catalytic effect • Catalytic effect of OH on epoxy-amine reaction	Park et al.[17]

As seen in Table 1, several studies focused on the effect of graphene materials on the cure behaviour of epoxy resins. It is clear from the table that all these studies have been carried out based on DSC technique. Nevertheless, it can be seen that there are discrepancies in outcomes among different research groups. Similarly, both accelerating and retardation effect of carbon nanotubes (CNTs) on different epoxy systems have been reported [24,36-38]. The disparity in results suggests that the epoxy-GO; epoxy-graphene or epoxy-CNT reactions are sensitive to the detailed chemistry of the epoxy resin system (especially the nature of the curing agent) as well as the functional groups on the surface of the carbon nanoparticles. A

rationalization of these contradictory results may possibly be found in the work of Putz et al.[20] on carbon nanotube-epoxy composites. They found that two opposing effects may be seen: network disruption at the nanotube-polymer interface lowering T_g and formation of an interphase in which chain dynamics were retarded leading to a higher T_g. However, the conflicts may reflect the limitations of the DSC technique itself.

Although the kinetics of cure reaction has been widely studied by DSC, the technique does not generally provide chemical information and detailed mechanism of the cure process and in particular the chemistry of the interphase region between resin and reinforcement [39]. One of the major limitations of DSC is that it is a bulk measurement and if the graphene or GO sheets are not fully exfoliated then changes in the heat flow due to reaction of the functional groups in the interphase with the bulk epoxy resin and curing agent are going to be small. If the system is exfoliated and has a high surface area then DSC is a useful method for studying changes in cure exotherm and T_g, but an assumed order of reaction is required to generate kinetic data with non-isothermal studies at different heating rates being particularly problematic. Isothermal studies are therefore preferred when cure reactions are studied.

The FT-IES method described here offers an alternative analytical approach to monitor the chemical reactions and mechanisms throughout the curing process. Emission of infrared radiation occurs from all bodies at ambient temperature and may be imaged with IR cameras, but in most cases the spectral information is lost due to reabsorption of the radiation and temperature gradients within the body. When the emitter is a thin film, reabsorption and temperature gradients are minimized and IR emission spectra equivalent to IR absorption may be obtained [22]. The emission intensity is weak at room temperature due to the low population of the higher vibrational states, but at the cure temperatures of many resin-hardener systems ($\geq 100^{o}$C) there is a significant intensity in the "fingerprint" region of the IR spectrum so that the cure chemistry may be followed in real time. Use of the technique on very thin film samples gives an added advantage of offering the information on the interphase region where molecular chemical reactions occur during the curing process. Because of the specialized nature of the technique, limited investigation of amine curing of epoxy resin based on IR emission has been reported. George et al.[22] reported a detailed kinetic study on the curing of TGDDM/DDS epoxy mixture transferred as a thin film from the surface of carbon fibre-epoxy prepregs. They observed the spectral changes during cure which were used to monitor the chemical changes and to study the

cure kinetics. For example; decrease in both the 1° amine bending band at 1652 cm^{-1} and epoxy cyclic ether band at 906 cm^{-1} and increase and broadening of ether group at 1085 to 1140 cm^{-1} and hydroxyl group at 1000 to 1100 cm^{-1} were observed with the progress of cure. These observations are consistent with the sequence of reactions occurring during the cure (Fig. 1). Calculated activation energies (from Arrhenius plots) showed that homopolymerization is dominant in catalysed resin from epoxy prepregs compared to a model system where auto-catalysed 1° amine-epoxy reaction is favoured.

In this article, we wish to evaluate the influence of GO on the curing process and also to understand the chemical reaction mechanisms at the interphase of epoxy resin and GO during the curing process based on the FT-IES method. We further study the effect of OD on cure kinetics of epoxy. DSC studies were also conducted in parallel with the IR emission experiments for an independent measure of extent of reaction with time of cure and also the T_g of the system at different extents of reaction. We believe that this opens up a new approach to evaluate and understand curing behaviour and structure of epoxy nanocomposites, especially at the interphase.

2. EXPERIMENTAL

2.1. Materials and characterization

The materials used in this study were the commercial DGEBA resin (Diglycidyl ether of bisphenol A) and curing agent DDM (4, 4'-diamino-diphenylmethane). Typical structures of DGEBA and DDM are presented in Fig. 2.

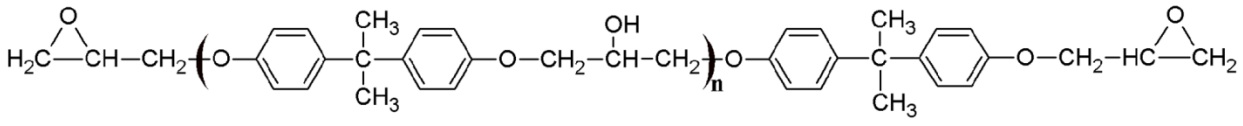

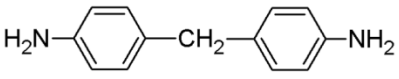

Fig. 2. Structures of DGEBA (typically, n=0.1) and DDM.

GO was prepared, following a modified Hummers method (supporting information) [40]. As produced GO (aGO) was purified and OD was isolated by an autoclave method which

avoided the complications of base washing. Autoclaved GO is called acGO hereafter. More details on synthesis and characterization of aGO, acGO and OD can be found in supporting information for this paper. aGO, acGO and OD were characterized by different microscopic methods such as SEM, TEM, AFM and spectroscopic methods: FTIR, Raman, (see supporting information). X-ray photoelectron spectroscopy (XPS) analysis was employed to detect oxygen contents and micro-chemical environment of aGO and acGO. XPS measurements were performed with a Kratos Axis ULTRA X-ray photoelectron spectrometer using monochromatic Al-kα radiation (hv = 1486.6 eV). CasaXPS v 2.3.16 software was used to perform curve fitting and to calculate the atomic concentrations. The surface area of the aGO was estimated by the methylene blue (MB) method reported by Navajas et al.[41] as detailed in supporting information.

2.2. IR emission study

To achieve thin films on the FT-IR emission hotplate, solutions of known concentration were deposited from dimethylformamide (DMF). The resin mixture was prepared by dissolving the required amounts of DGEBA and DDM (weight ratio of 2:1) in a small amount of DMF at room temperature. Resin mixture with GOs (aGO or acGO) was prepared by firstly exfoliating and suspending GO in the DMF (1mg/ml) by sonicating for 1 h and then adding the required amount of GO solution into the resin mixture at room temperature. GO content used in this study was 0.3 wt% in the total resin mixture which was chosen since it provides a homogeneous dispersion and most of previous work reported that the maximum property enhancement was achieved with a graphene or GO loading of 0.1 – 0.5 wt%.[6,15,16,18,19,42] In the case of OD, powdered OD isolated from the water after autoclave treatment of GO was dissolved in water and then added into DGEBA-DDM mixture in DMF. Water and DMF are completely miscible and gave a clear solution.

FT-IR emission analysis was performed with a Nicolet Nexus spectrometer equipped with a liquid N_2 cooled mercury cadmium telluride detector and an external graphite furnace emission accessory, described elsewhere [43]. The graphite furnace was fitted with either a platinum hotplate of 6 mm diameter or a graphite reference plate. 1 μl of uncured epoxy mixture in DMF was transferred by a micro-syringe on to the platinum plate, pre-heated to 100^{o}C to get a very thin film of the sample on the plate. The solvent evaporated immediately after putting the

sample on the platinum plate so there was no solvent interference in the sample spectra. IR emission spectra were collected under dry air immediately the sample was deposited and the solvent evaporated [22]. The average spectrum of 128 scans was obtained at spectral resolution of 4 cm^{-1}. Successive single beam spectra were collected at every 2 minutes for an initial 16 minutes and then every 5 minutes for a total cure time of 30 minutes.

To linearise the spectra with respect to concentration, equivalent absorbance spectra were calculated by exploiting the relationship between absorbance and emittance, $A \approx -\log(1-\varepsilon)$, where ε is the ratio of the sample signal to the graphite signal after accounting for the contribution of the clean Pt substrate and instrument background contributions. Spectra of different concentrations of DGEBA resin (10, 5, 2.5 and 1 mg/ml) were obtained to get the relationship between concentration and peak intensity.

2.3.DSC study

DSC study was conducted with a TA instruments Q100 differential scanning calorimetry. Samples were prepared following the similar procedure as described above using acetone as the solvent. This is because the lower boiling point of acetone facilitates the faster evaporation of the solvent at lower temperature, so avoiding premature cure of the resin-hardener mixture. Acetone was evaporated by stirring the epoxy resin at 40^{o}C for few hours on a hot plate with a magnetic stirrer. Then the hardener was mixed and the mixture was placed under vacuum at the same temperature for further 1 hour for the complete removal of solvent. A series of DSC samples were prepared by adding ~5 mg into the hermetic type DSC aluminium pans which were thermally equilibrated in an oven at 100^{o}C. Each sample was partially cured by removing them from the oven at different time intervals (0, 5, 10, 15, 20, 25 and 30 minutes). The heated samples were immediately put in the deep-freezer to stop the reaction. Then, the heat flow curves were obtained for each sample at a scanning rate of 10^{o}C/min from 20 to 200^{o}C under nitrogen atmosphere. The total heat of reaction (ΔH_o) was calculated using the heat flow curve for the system before curing at 100^{o}C and the conversion of the cure reaction (α) was determined at each time, t, as $\left(1-\frac{\Delta H_t}{\Delta H_o}\right)$; where ΔH_t is the heat of reaction after cure for time t at 100^{o}C.

3. RESULTS AND DISCUSSION

3.1.Characterization of aGO and acGO

aGO, acGO and OD prepared in this study were characterized by several spectroscopic and microscopic techniques prior to fabricating the nanocomposites. Estimated surface area of aGO is 719 m^2/g as determined by methylene blue binding (supporting information, Fig 5s) which is comparable to values reported in literature [12,41].

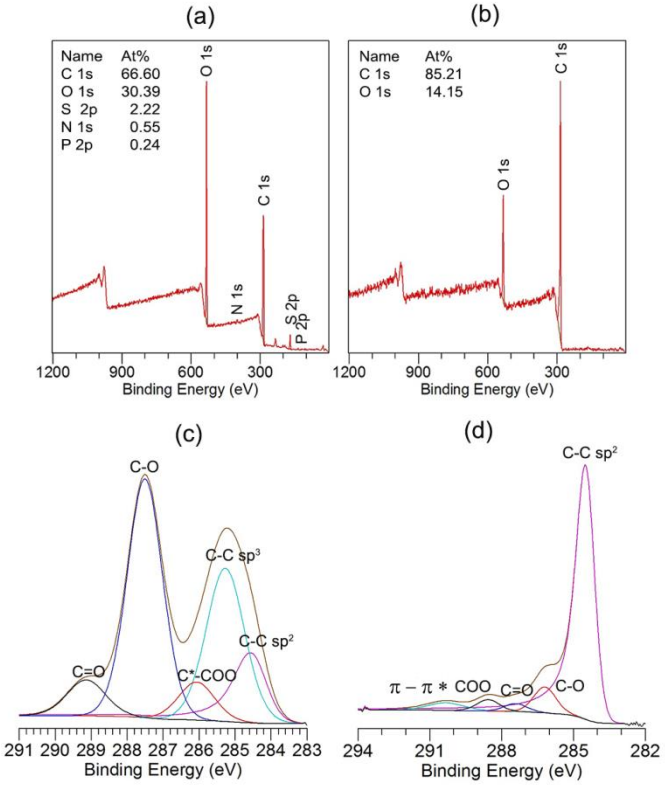

Fig. 3. XPS survey spectra of (a) aGO (b) acGO; C 1s XPS multiplex spectra of (c) aGO and (d) acGO. Note the large decrease in oxygen content after autoclaving and OD removal.

XPS analysis was employed to detect oxygen content and surface chemical environment of aGO and acGO. The atomic composition of aGO and acGO was obtained from survey spectra (Fig 3(a) and (b)) and revealed that aGO contains 66.6 atom% of carbon and 30.4 atom% of oxygen. The remaining elements in aGO are nitrogen (0.55%) sulphur (2.2%) and phosphorus (0.25%) which arise from the original graphite and the Hummer's method of synthesis. The oxygen content decreased to 14.2 atom% and carbon increased up to 85.2 atom% in acGO after

autoclave treatment, giving O/C ratio of 0.46 for aGO and 0.17 for acGO in good agreement with earlier work on base washing of GO [7,44-47]. This confirms the removal of oxygen functional groups during the autoclave cleaning process, but the question remains as to whether the aGO has been chemically reduced or the surface has just been cleaned. Deconvolution of XPS multiplex spectra and assignment of bands requires first the determination of a reference band which is usually chosen to be sp^3 carbon 1s at 285eV. However in the case of graphite and graphene with predominantly sp^2 hybridisation, the band shifts to 284.3eV and there is an asymmetric band shape tailing to higher binding energy as seen in the spectrum of the starting graphite material used in this study (supporting information, Figure 1s).

The multiplex C1s spectrum of aGO was deconvoluted by using five peaks assigned to non-oxygenated C (sp^2, 284.6 eV and sp^3, 285.3 eV), C attached to COO (C*-COO, 286.1 ev) epoxy, hydroxyl and carbonyl groups (C−O and C=O ∼287.5 eV), and carboxylate groups (COO, 289.1 eV) (Fig 3 (c). In contrast the XPS spectrum of acGO shows one main peak at 284.5 eV (C=C, sp^2), and four small peaks at 286.2 eV, 287.4 eV, 288.5 eV and 290.3 eV. These peaks can be assigned to C-O, C=O, O-C=O and a π-π shake-up band, respectively (Fig 3(d)) [45]. However, the oxidation peaks are considerably smaller compared to those of aGO which indicate that the quantity of oxygen moieties in aGO decreases after the removal of OD. In comparison, a similar reduction of degree of oxidative functionality was reported for bwGO [7,48,49]. Rourke et al., found that O/C ratio reduced from 0.5 in aGO to 0.25 in bwGO [7]. In summary, our XPS data on acGO is comparatively close to that reported for bwGO except that the removal of OD appears to be more efficient, as given by the appearance of the π-π shakeup band which is a characteristic feature of graphene that is not seen in aGO. It has been suggested in one other study that reduction has occurred [50] on an autoclave treatment in water but it is generally regarded that chemical reduction by high temperature treatment with hydrogen or hydrazine is necessary to restore characteristic graphene properties such as conductivity[51]. This study of acGO clearly shows that there are some graphene-like properties eg. The return of a black colour indicating higher conjugation; the failure of the acGO to disperse in water; the reduction of the interlayer spacing from 0.82 nm in aGO to 0.35 nm in acGO (XRD data, supporting information Figure 2s) as well as the evidence for sp^2 hybridisation in the C1s XPS band. However there are sufficient oxidized groups still retained on the surface to allow dispersion of acGO in DMF, unlike pure graphene.

The dispersibility of acGO (as well as aGO and OD) in DMF allows the intimate mixing with epoxy resin (DGEBA) and curing agent (DDM) and deposition of thin films for infrared emission studies of the change in functional group concentration during cure of DGEBA with DDM at 100^{o}C.

3.2. IR emission study

The raw emission spectra, all collected at 100^{o}C, necessary to determine the equivalent absorbance spectrum of DGEBA-DDM are shown in the Fig. 4. These are, from top to bottom:

1. A graphite black body
2. A thin film of uncured DGEBA-DDM on the platinum hotplate
3. The clean platinum hotplate

The lowest (green) curve in Fig. 3 represents the emission spectrum of DGEBA-DDM at 0 min cure, shown in calculated absorbance units.

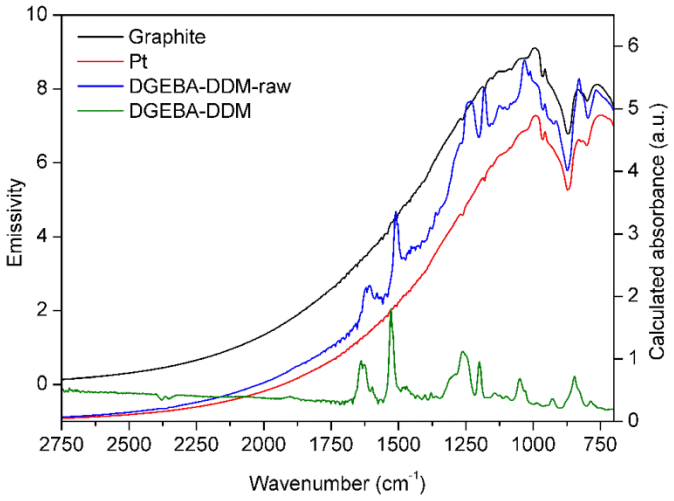

Fig. 4. IR emission spectra at 100 ^{o}C of (from the top): graphite reference plate; the DGEBA-DDM sample on the platinum plate; the clean platinum plate and the equivalent absorbance spectrum of the sample (right axis), calculated from these emissivity curves.

As an illustration of the quantitative aspects of the FT-IES analysis, different layers have been deposited of DGEBA resin without curing agent but at different concentrations in DMF. In each case 1µl of solution was deposited and as shown in Fig. 5, the peak heights scale as expected for films of thickness corresponding to 0.5, 0.25, and 0.1 times the original thickness. Further, this also indicates that the calculated absorbance scale is quantitative with respect to

concentration so can be used for kinetic studies of cure. The calculated thicknesses range from 1150 nm to 115 nm which illustrates the sensitivity of the technique for studying the cure chemistry of the interphase with even partial exfoliation. It should be noted that in some runs there are unavoidable traces of water vapour in the sample compartment that result in underlying bands that may appear positive or negative after ratioing to the platinum reference spectrum in the region from 1800cm^{-1} to 1500 cm^{-1}. These do not affect the quantitative analysis of the resin components.

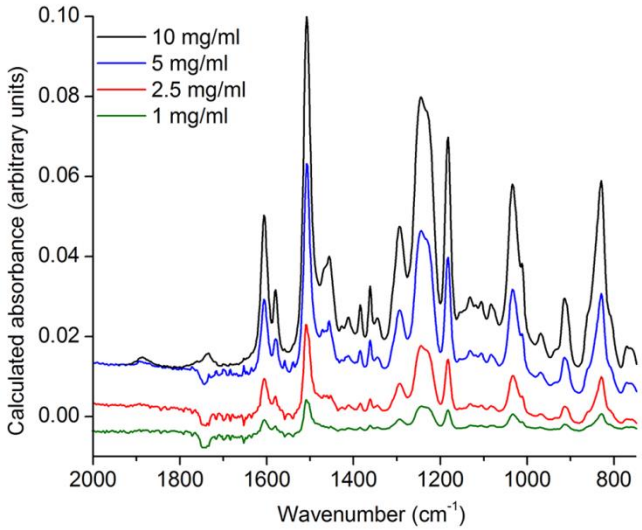

Fig. 5. FT-IR emission spectra of thin films of DGEBA at 100 ^{o}C after deposition of 1µl of DMF solution of concentration (from top to bottom curves); 10 mg/ml; 5 mg/ml; 2.5 mg/ml and 1 mg/ml.

Table 2

List of functional and reference bands (used to normalize functional bands) of the DGEBA-DDM system used for the cure study

Functional band	Wavenumber (cm^{-1})	Reference band (Used for Normalization)	Wavenumber (cm^{-1})
N-H bend (1°amine)	1621	C-H bend/ Benzene ring stretch	1511
N-H wag (1° & 2° amine)	768	C-H wag	1180
Epoxy ring stretch	914	C-H wag	1180
Ether	1100	C-H wag	1180

IR emission spectra of DDM, DGEBA and DGEBA-DDM are shown in Fig. 6 and the functional group and reference bands that have been used for the cure study are tabulated in Table 2.

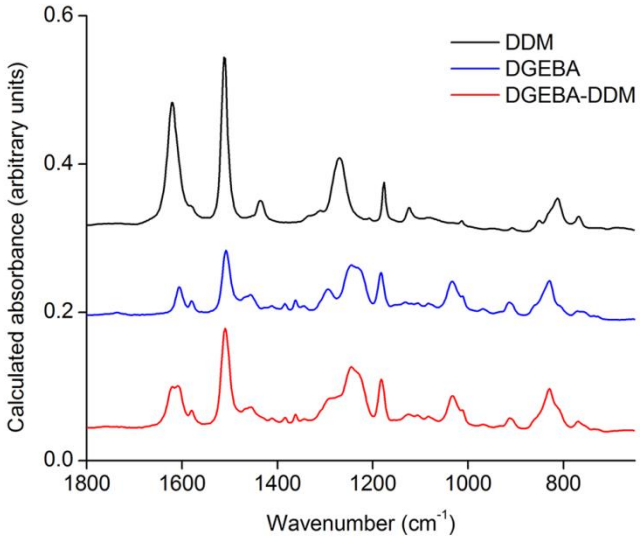

Fig. 6. IR emission spectra (from top to bottom curves) of DDM, DGEBA and DGEBA-DDM (at the weight ratio of 2:1) at 100^{o}C

3.2.1. Emission spectral changes during cure of DGEBA-DDM

Fig. 7 shows a series of 12 successive spectra obtained continuously during the curing of neat epoxy resin at 100^{o}C under dry air for 30 minutes. The spectrum at 0 min. represents the different functional groups of both epoxy resin and curing agent at the start of curing. The subsequent spectra show the emission curves at different stages of curing. The first spectrum is noisier in the region 2000 cm^{-1} to 1400 cm^{-1} compared to rest of the spectra. This is due to the effect of atmospheric moisture which may flow into the testing chamber on opening of the chamber for sample insertion. The moisture effect disappeared in the following spectra with continued flushing of dry air into the chamber. The spectral changes during the curing can be clearly seen from the stacked spectra.

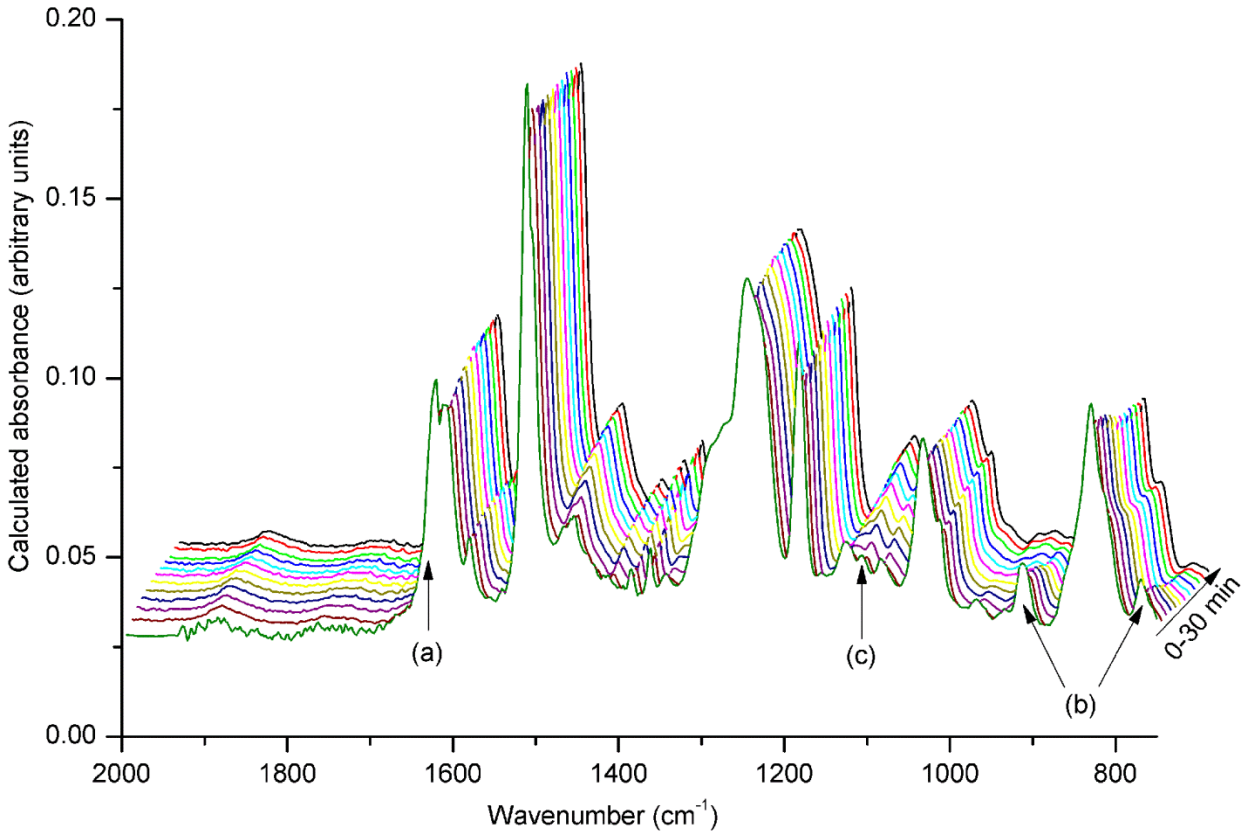

Fig. 7. Stack plot of successive spectra of DGEBA-DDM at 100 ^{o}C for cure up to 30 minutes. The bands labelled (a), (b) and (c) are shown expanded in Fig. 8.

The sharp peak (a) at 1621cm^{-1} is due to NH bending of the 1° amine band of DDM. This peak decreased rapidly with heating as it can be seen in the expansion plots of spectra in Fig. 8 (a). Similarly, epoxy peak at 914 cm^{-1} and NH wag band at 768 cm^{-1} diminished significantly with the progress of curing (Fig. 8b). Decrease of peak intensities indicates the consumption of the amine and epoxy functional groups to form the 3D network structure during the curing process but more detailed analysis is required to separate the individual reactions 1 to 3 in Fig. 1. Further, we observed the increase and broadening of peak at around 1100 cm^{-1} (Fig. 8c) which is consistent with the formation of ether groups by etherification reaction between hydroxyl and epoxy (Fig. 1, reaction 3) and homopolymerization. Table 2 shows the peaks that change during cure and the band assignments. Similar spectral changes during the amine curing of epoxy systems have been reported in literature [22,52].

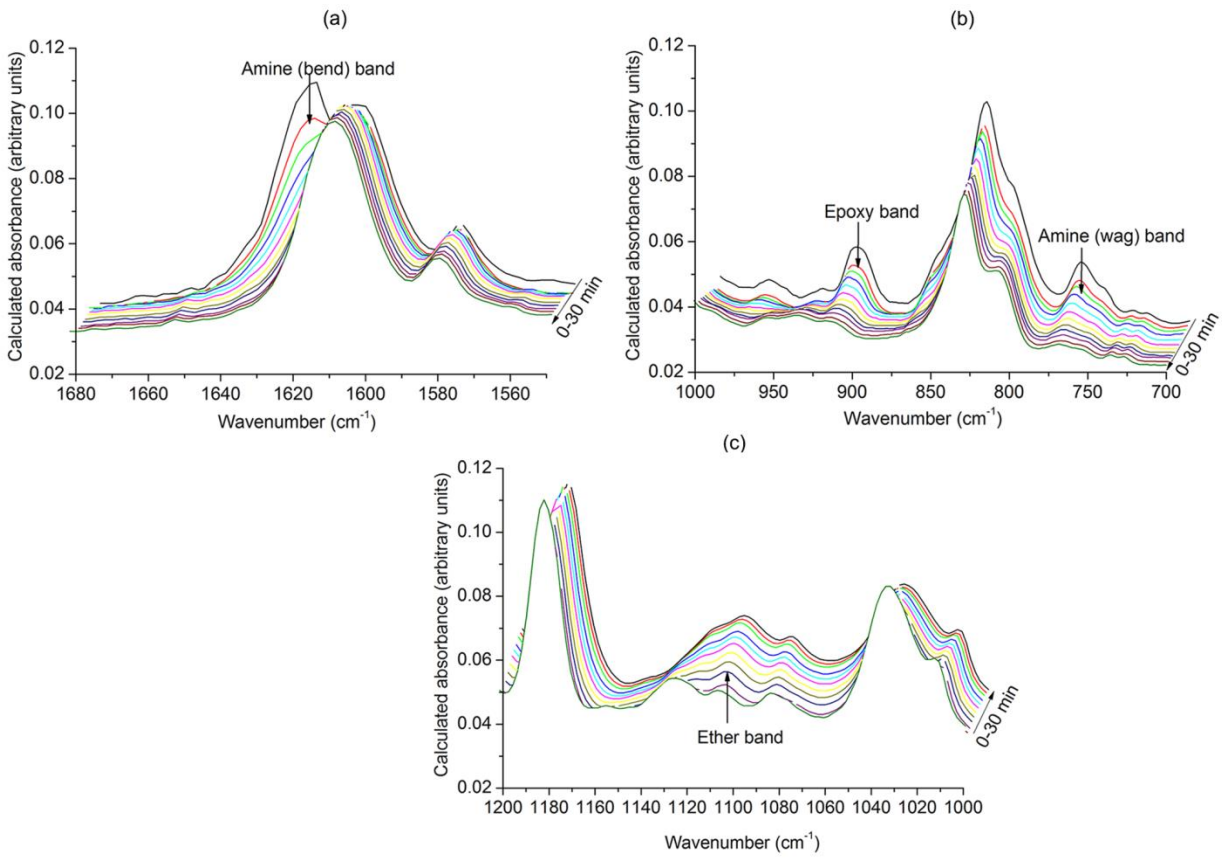

Fig. 8. Expanded and reoriented stack plot of successive spectra of Fig 7., showing (a) consumption of 1° amine as change of N-H bend band (b) consumption of epoxy and N-H wag of 1° and 2° amine band (c) growth of ether band.

To investigate the influence on epoxy resin cure chemistry of as-prepared and autoclaved GOs (aGO and acGO, respectively) and the OD obtained after autoclaving, the cure kinetics of DGEBA-DDM nanocomposites were studied using the same experimental conditions at GOs or OD loading of 0.3wt%. Similar spectra and spectral changes were observed as shown in the supporting information, Fig. 6s, but it was apparent that the rates of the reactions of the species responsible for the spectra have changed when compared to the bulk resin. These changes are attributed to the influence of GOs on the detailed cure chemistry. Since the emission intensity bands when converted to absorbance are proportional to the concentration of the species, spectral manipulation allows the time-dependent concentration profiles of epoxide, 1° amine and 2° amine to be monitored with time of cure and instantaneous reaction rates determined.

3.2.2. Influence of GOs on the cure reactions of DGEBA-DDM from IR emission spectra

The cure kinetics and the effect of GOs and OD addition on the curing process were determined by analysis of the spectral changes in different nanocomposite systems. Figs. 9 and 10 display the change of band intensities due to the epoxy group from normalized spectral peak area at 914 cm^{-1}, amine groups determined by normalized spectral peak area at 1621cm^{-1} (N-H bend) and 768cm^{-1} (N-H wag) and the ether group from normalized spectral peak area at 1100 cm^{-1} in the epoxy resin and its nanocomposites. Peak normalization was done by dividing those bands with the reference bands given in Table 2 at the same curing time. The band intensity changes arise from the chemical reactions shown in Fig. 1 and the instantaneous slopes of the lines in Figs. 9 and 10 reflect the rate of these reactions during cure. It is clear that 1° amine and epoxy groups gradually decrease in concentration during resin cure, due to epoxy-amine addition (Fig. 1, reaction 1), which has been reported as the dominant reaction up to gelation [22,23].

3.2.2.1. Epoxy consumption including etherification reaction

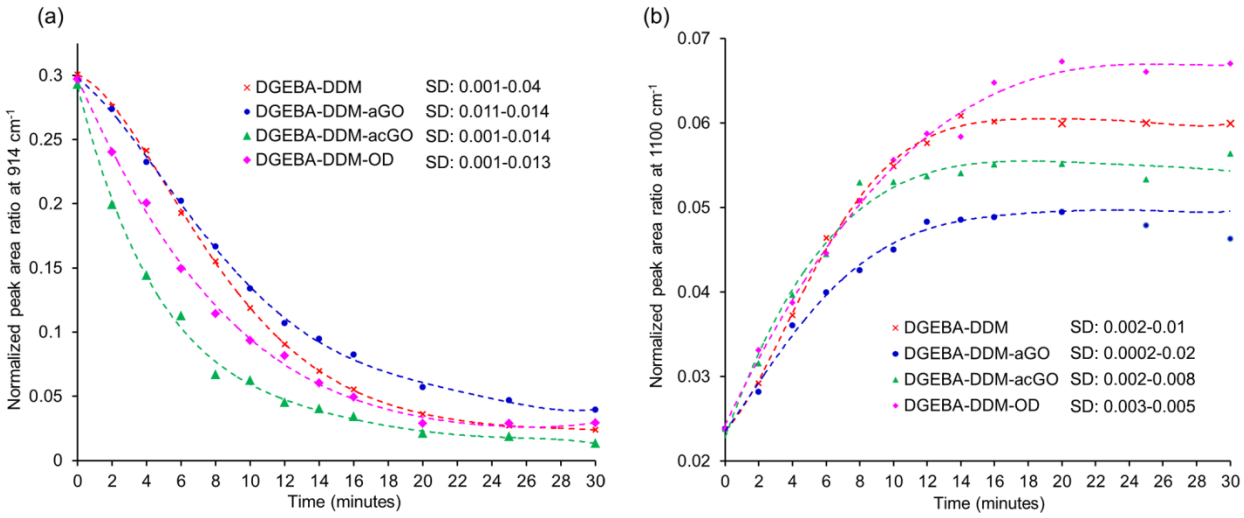

Fig. 9. (a) Consumption rate of epoxy group at 914 cm^{-1} and (b) formation rate of ether group at 1100 cm^{-1} during cure at 100 °C of DGEBA-DDM (-x-/red), DGEBA-DDM-aGO (-•-/blue), DGEBA-DDM-acGO (-▲-/green) and DGEBA-DDM-OD (-⬩-/pink). All data were normalized with initial value of DGEBA-DDM for comparison. Dashed lines represent the trendline of the individual curves. SD values show standard deviation for each system.

The rate of epoxy consumption by the reactions with amine shown in Fig. 1, reaction 1 to 3 is given by equation 5.

$$-\frac{d[\triangle]}{dt} = k_1[\triangle][1°A] + k_2[\triangle][2°A] + k_3[\triangle][3°A] \quad (5)$$

It is important to note in Fig. 9(a) that compared to neat DGEBA-DDM, aGO-epoxy nanocomposite shows a slower rate of epoxy group consumption whereas acGO-epoxy and OD-epoxy systems exhibit faster rate of epoxy consumption. The consumption of epoxy is autocatalytic in both the neat DGEBA-DDM resin and the nanocomposite with aGO (as seen by the slower initial rate) but this is not seen from samples containing either OD or acGO. This suggests that both of these contain catalytic sites that enhance the ring-opening of the epoxy.

The rate of epoxy consumption with amine is given by equation 5. The initial epoxide consumption rates, $-d[\triangle]/dt_{(initial)}$, calculated from data before normalization are given in Table 3 and are 0.037 $Amin^{-1}$ and 0.022 $Amin^{-1}$ for acGO nanocomposite and OD system respectively, where A is the peak area ratio in Fig. 9(a) which is proportional to epoxy concentration. These values may be compared to 0.01 $Amin^{-1}$ from the neat DGEBA-DDM system indicating that there is a clear change in reaction mechanism in the presence of acGO and OD.

Table 3

Initial rates of epoxy and 1°A amine consumption from FT-IES band areas

System	$-d[\triangle]/dt_{(initial)}$ $Amin^{-1}$	Rate, r, relative to DGEBA-DDM	$-d[1°A]_{initial}/dt$ $Amin^{-1}$	Rate, r, relative to DGEBA-DDM
DGEBA-DDM	0.01	1.0	0.049	1.0
acGO	0.037	3.7	0.079	1.61
aGO	0.01	1.0	0.043	0.88
OD	0.022	2.2	0.029	0.59

As shown in Fig. 1, during each epoxy ring-opening reaction, a hydroxyl group is formed. Another epoxide group may then react with this hydroxyl group (equation 4) to form an ether group. A further epoxide reaction is homopolymerization which also creates ether linkages and is catalysed by tertiary amines or Lewis acids [22,53]. However, it is reported that in the absence of catalyst, hydroxyl-epoxide reaction or homopolymerization are less likely to occur at

the early stage of curing [22]. However, etherification is occurring as seen from the growth in the band at 1100cm^{-1} as plotted in Fig. 9(b).

Etherification results (Fig. 9b) showed a faster reaction of acGO and a slower reaction of aGO nanocomposites compared to neat DGEBA-DDM resin. Importantly, the OD-system has a faster rate of formation and a higher concentration of ether groups than that of neat DGEBA-DDM resin which is consistent with the epoxy consumption rates being due in part to a higher extent of etherification in the presence of oxidized debris. Further support for etherification enhancement in OD system is found later in the slower rate of epoxy-amine reaction compared to neat resin (Table 3 and Section 3.2.2.2) where the competing reactions are discussed in more detail.

3.2.2.2. 1° amine - epoxy reaction

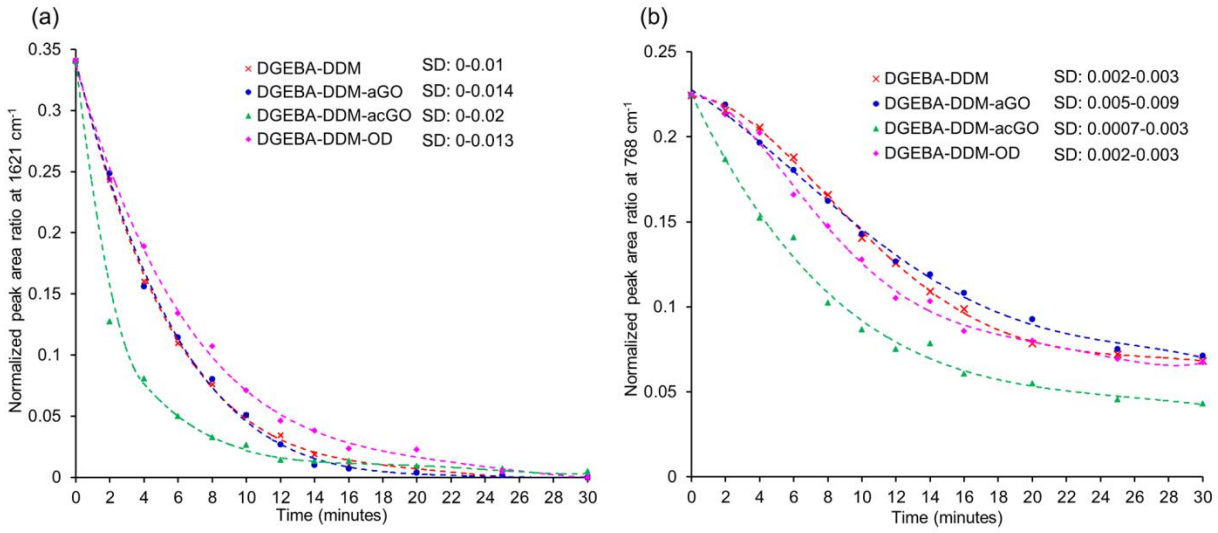

Fig. 10. Consumption rate of (a) 1° amine (N-H bend) at 1621 cm^{-1} (b) 1°/2° amines (N-H wag) at 768 cm^{-1} during cure at 100 ^{o}C for 30 minutes of DGEBA-DDM (-x-/red), DGEBA-DDM-aGO (-•-/blue), DGEBA-DDM-acGO (-▲-/green) and DGEBA-DDM-OD (-⬩-/pink) All data were normalized with initial value of DGEBA-DDM for comparison. Dash lines represent the trendline of the individual curves. SD values show standard deviation for each system.

The change in the normalized peak area of 1° amine N-H bending at 1621cm^{-1} is similar for both neat epoxy resin and aGO nanocomposite throughout the curing process (Fig. 10a). In contrast, acGO nanocomposites show significantly faster decrease in 1621cm^{-1} band while the OD system shows a slightly slower decrease compared to the neat DGEBA-DDM during cure.

The initial rate of 1°amine consumption of DGEBA-DDM-aGO is very similar to that from DGEBA-DDM, so this suggests there is no contribution from reactive groups on the aGO such as surface epoxides. From the initial change of 1° amine from Fig. 10(a), the initial rates (as $-d[1°A]_{initial}/dt$) values can be calculated and are shown in Table 3. A is the normalized 1° amine band area from the FT-IES spectrum which is proportional to [1°A]. An important result in Table 3 is that the rate of reaction of 1° amine in the presence of OD is only 59% of that of the neat resin which suggests that it is the oxidative debris that is suppressing the reactivity of the aGO. The ratio of rates: $r_{(acGO)}/r_{(aGO)}$ is 1.84 which means that removal of OD increases the 1° amine consumption rate by 84% which may reflect the recovery of a catalytic effect of the "clean" surface of acGO on removal of OD. The catalysis is apparent since as shown in Table 3, $r_{(acGO)}/r_{(DGEBA-DDM)}$ is 1.61.

From Table 3, OD shows a faster initial rate of epoxy consumption compared to the neat DGEBA-DDM in spite of the slower rate of amine consumption noted above. This suggests that OD may induce the ring opening reaction of epoxide in the system i.e. homopolymerization is favoured. Proposed ring opening reaction and homopolymerization are schematically shown in Fig. 11. It is believed that acGO is not favouring homopolymerization since there is faster consumption of 1° amine than aGO and also the 2° amine reaction is not suppressed to the extent that it is in aGO (Fig. 10b), which is discussed in more detail in Section 3.2.2.3.

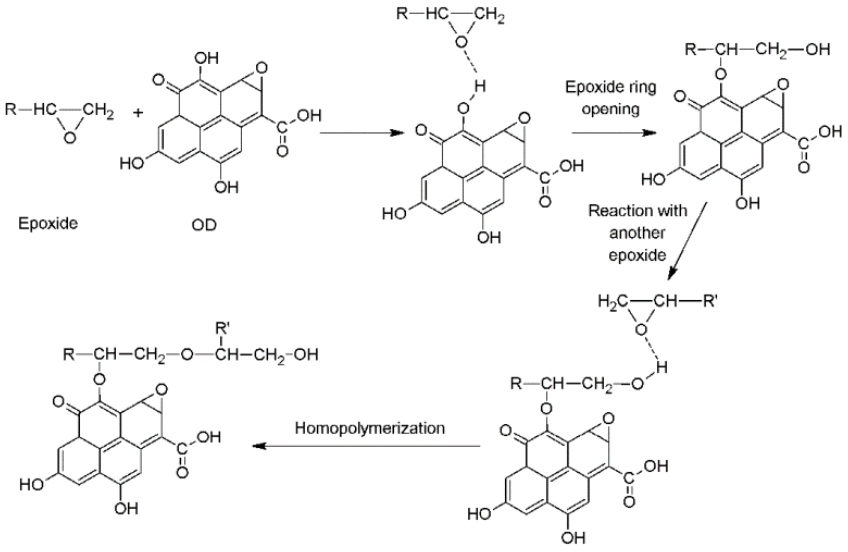

Fig. 11. Schematic of effect of OD on epoxy homopolymerization

OD represents about 14-30% of total mass of aGO and is strongly adhered to the graphene oxide surface [7,8]. This adhered OD can physically cover the active sites (eg; bound epoxide groups, hydroxyl groups, defects etc.) on GO surface which would act as reactants or catalysts of epoxide-amine reaction. As shown in the XPS studies (Section 3.1) removal of OD exposed these active groups which can actively participate in catalysing epoxide-amine reactions or reacting directly with amines, resulting in faster epoxide-amine reaction and consequently, higher consumption of 1° amine. Mauro and co-workers performed a DSC-based investigation to elucidate the catalytic activity of graphene based nanofillers on epoxy curing reaction [34]. They observed that graphene or GO is able to catalyse the epoxide-amine reaction and catalytic effect can be on both reactions between 1°amine and epoxide as well as reactions between 2°amine and epoxide groups. It is also well known that graphene and GO have catalytic effects on several other organic reactions [47,54,55]. In those studies the catalytic effect of base washed (OD-free) GO on aerobic oxidative coupling of 1° amines was evaluated and compared with as-produced GO and OD [47]. It was shown that OD-free GO has significant catalytic activity with oxidative coupling product of 89% compared to lower catalytic effect of controlled aGO and OD samples (44% and <2% yield, respectively). It was suggested that the synergistic catalytic effect originates from combination of greater access to the catalytic sites by the reactants including exposed carboxylic acid groups and unpaired electrons at the edge defects with the removal of OD [47].

3.2.2.3. 2^o amine formation and reaction

As noted above in Section 3.2.2 and Fig. 8(b), the peak at 768cm^{-1} is due to N-H wag of both 1° and 2° amines [53]. The contributions of the concentration of the 1° amine to the band intensity (from the 1° amine bend band at 1621 cm^{-1}) may be subtracted and the change in concentration of 2° amine during cure determined from equation 6:

$$A_{NH\ wag} - aA_{NH\ bend} = b[2°A] \quad (6)$$

Where;

$A_{NH\ wag}$ = Normalized peak area ratio of NH wag band

$A_{NH\ bend}$ = Normalized peak area ratio of NH bend band

[2°A] = Concentration of 2° amine

a, *b* = Constants related to the molar absorptivity of the bands analysed

a is determined from the spectrum at 0 minute. At 0 min, [2°A] = 0, Therefore, $a = \frac{A_{NH\ wag}}{A_{NH\ bend}}$

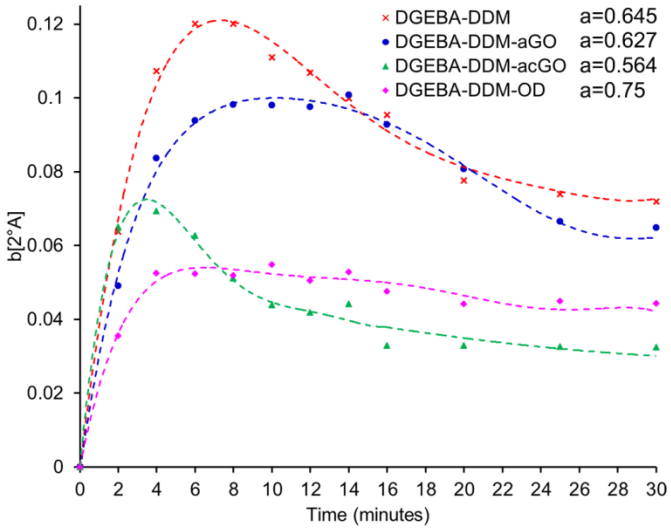

Fig. 12. Calculated 2° amine concentration from emission spectra during the cure of DGEBA-DDM (-x-/red), DGEBA-DDM-aGO (-•-/blue), DGEBA-DDM-acGO (-▲-/green) and DGEBA-DDM-OD (-⬩-/pink) at 100 ^{o}C for 30 minutes. Dash lines represent the trendline of the individual curves. The calculated values of the parameter "a" for each system are shown in the plot.

The calculated parameter b[2°A] has been plotted against the curing time for the 4 different systems in Fig. 12. The formation of 2° amine occurs from the onset of cure due to the reaction of epoxide with 1° amine group and this concentration increased rapidly at early stages of curing (Fig. 1, reaction 1). The 2 amines can further react with epoxide groups forming 3° amine (Fig. 1, reaction 2) which results in formation of the 3D network structure in the resin matrix. Therefore there is a consecutive reaction of creation and consumption of 2° amine as seen by the growth to a maximum in Fig. 12. Then, depending on the relative magnitude of the rate coefficients for 2° and 3° amine formation this profile will change.

For consecutive second order reactions, at the maximum [2°A] at time t, then $\frac{d[2°A]}{dt} = 0$

So, from Fig. 1- equation 2, $k_1[1°A][\triangle\!\!\!\!\circ] = k_2[2°A][\triangle\!\!\!\!\circ]$

Hence, at this point:

$$\frac{k_1}{k_2} = \frac{[2°A]_t}{[1°A]_t}$$

and in principle the ratio of rate coefficients of 1° and 2° amine reaction with epoxide, k_1/k_2, could be determined from the data in Figs. 10(a) and 12. However, as may be seen from Figure 12, the plot is of b[2°A] against time so there is an unknown constant, b, due to the unknown molar absorptivity of the species being measured in the FT-IES spectra. In spite of this limitation it is possible to calculate the rate coefficient, k_2, for each system relative to the neat epoxy resin in the way shown below to give an empirical value $k_{2(rel)}$. Table 4 shows the calculated ratios bk_1/k_2 for four systems from the data in Figs. 10(a) and 12 taken at the maxima of the curves in Fig. 12 together with the calculated $k_{2(rel)}$ using these results plus the relative rate of 1° amine consumption compared to neat DGEBA-DDM in Table 3.

Table 4

Calculated ratio bk_1/k_2 and the rate coefficient $k_{2(rel)}$ of 2° amine reaction in the system relative to that in neat DGEBA-DDM resin

System	bk_1/k_2	$k_{2(rel)}$
DGEBA-DDM	1.33	1.00
DGEBA-DDM-aGO	2.13	0.55
DGEBA-DDM-acGO	1.15	1.40
DGEBA-DDM-OD	1.21	0.49

A sample calculation of $k_{2(rel)}$ is given below for the system DGEBA-DDM-aGO.

$$\frac{bk_{1(DGEBA-DDM-aGO)}/k_{2(DGEBA-DDM-aGO)}}{bk_{1(DGEBA-DDM)}/k_{2(DGEBA-DDM)}} = \frac{2.13}{1.33} = 1.60 = \frac{bk_{1(DGEBA-DDM-aGO)}}{bk_{1(DGEBA-DDM)}} \times \frac{k_{2(DGEBA-DDM)}}{k_{2(DGEBA-DDM-aGO)}}$$

Since the ratio of the 1° amine consumption rate for DGEBA-DDM-aGO to that for DGEBA-DDM is given in Table 3 as 0.88 then:

$$\frac{k_{2(DGEBA-DDM)}}{k_{2(DGEBA-DDM-aGO)}} = \frac{1.60}{0.88} = 1.82 = 1/k_{2(rel)}$$

Therefore the rate coefficient of 2° amine reaction in aGO nanocomposite compared to neat resin is 0.55. The other values of $k_{2(rel)}$ in Table 4 may be determined in the same way.

It was hypothesised that the slower consumption of 2° amine in aGO could be attributed to two factors ie; covering of reactive sites by OD and steric hindrance arising from the GO sheets themselves. The steric hindrance can occur when aGO, after reaction with one 1° amine group will be sterically hindered for reaction of the formed 2° amine with another epoxy group owing to the bulky structure of aGO. However, considering the close similarity of the $k_{2(rel)}$ values for the DGEBA-DDM-OD system and the DGEBA-DDM-aGO nanocomposite (Table 4) the difference in the rate of 2° amine reaction is mainly accounted for by physical covering of epoxy groups in aGO by adhered OD in a similar way as for the 1° amine-epoxide reaction. In addition if steric hindrance was a factor, slower consumption of 2° amine would be expected in DGEBA-DDM-acGO nanocomposite as well but we actually observed faster consumption in that system. So, it tells us that the steric hindrance effect is not dominant and greater effect would have arisen from the hiding of active sites by OD.

Of importance in this discussion is the point at which the resin gels since the 2^o amine-epoxide reaction may then become diffusion controlled. The gel time for DGEBA-DDM at the amine to epoxy ratio used here is reported to be 20 min at 100^oC [56]. The considerable slowing in 2° amine reactivity seen in Fig. 12 from all systems is occurring before the time for the onset of gelation and is considered to arise from the chemical differences between the systems rather than diffusion control.

2.3.2.4. 3^o amine formation

The comparative reactivity of the 2° amine groups (Fig. 1, reaction 2) in the bulk resin and the interphase may be assessed by computing the concentration-time profiles of 3° amine arising from the difference between the concentrations of 1° amine and 2° amine at each time during cure using equation 7.

$$a[3°A]_t = [1°A]_0 - [1°A]_t - b[2°A]_t \quad (7)$$

It is noted that the results presented in Figs. 9 and 11, the emitted IR radiation will be occurring from both the resin that is within the interphase region as well as from any “bulk” resin

away from the interphase. We have calculated the interphase fraction of aGO-epoxy nanocomposite based on the aGO addition of 0.3 wt% and an interphase thickness of 118 nm [11]. The interphase fraction is calculated as 30% (based on a cured resin density of 1.16 g/cm^{3}and the measured surface area of 719 m^2/g, given in supporting information).

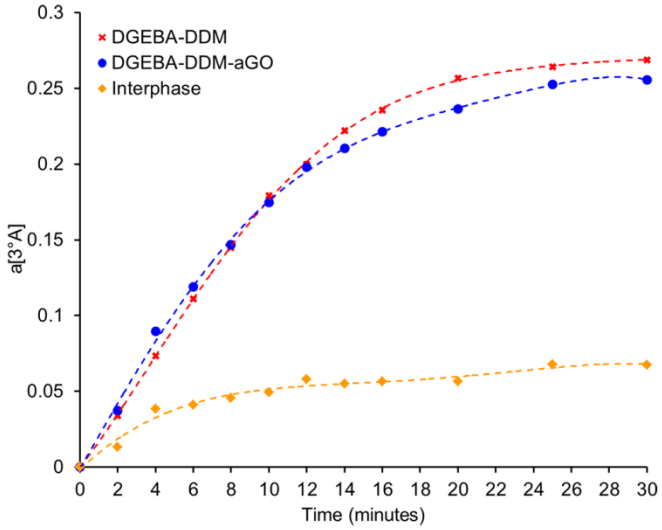

Fig. 13. Calculated 3° amine concentration during the cure at 100^{o}C for 30 minutes of DGEBA-DDM (-x-), DGEBA-DDM-aGO (-•-) and the interphase DGEBA-DDM-aGO based on 30% interphase contribution from surface area measurements (-⋆-). Dashed lines represent the trendline of the individual curves.

Fig. 13 shows the 3° amine profiles for the two systems DGEBA–DDM and DGEBA-DDM-aGO computed from the FT-IR emission intensities in Figs. 10(a) and 12. As discussed above, the profile measured for the DGEBA-DDM-aGO system comprises 70% from the bulk and 30% from the interphase. By allowing for this "bulk" contribution the 3° amine profile from the interphase region may be computed using equation 8 as shown below and is also shown in Fig. 13.

$$a[3°A]_{Interphase} = a[3°A]_{DGEBA\text{-}DDM} - 0.7\,(a[3°A]_{DGEBA\text{-}DDM\text{-}aGO}) \quad (8)$$

This profile is particularly interesting as it shows that the 2° amine reaction to produce 3° amine in the aGO-epoxy resin interphase is significantly retarded compared to the bulk resin with the reaction significantly slowing after the first 10 minutes of cure. This will result in a much lower crosslink density of the network in the interphase region since it is the 2° amine

reaction to produce 3° amine that results in the final reactivity and complete cure of the network. This will have consequences for the structure of the interphase since lower crosslink density will affect both T_g and the micromechanics, particularly toughness. Since diffusion control is occurring in both the neat resin and the interphase reactions only after 20 min of cure, this effect is in addition to any physical effects on the cure rate.

3.3. DSC study of extent of cure and T_g

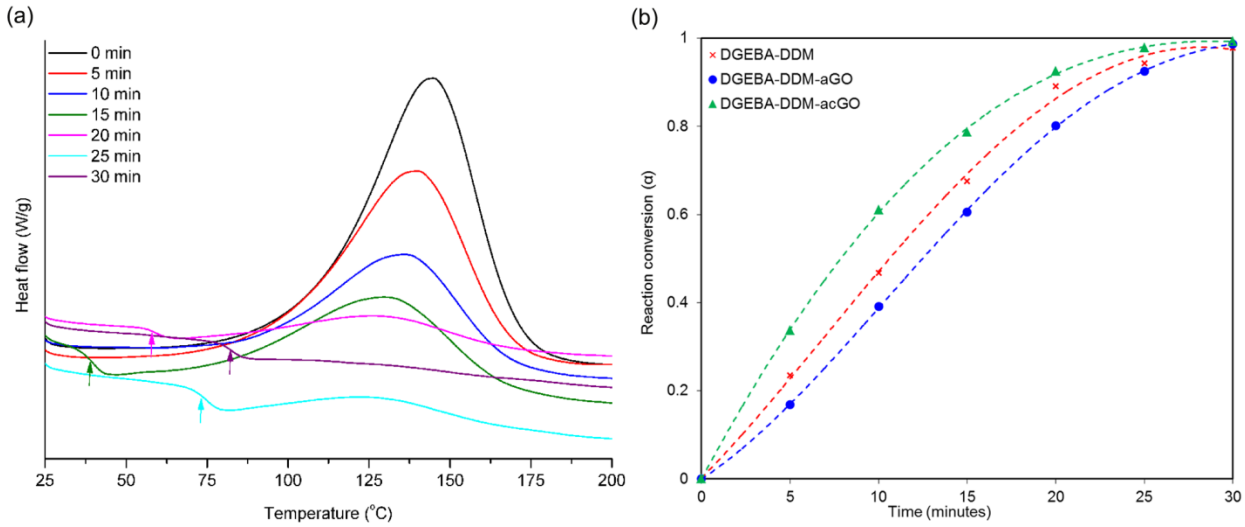

Fig. 14. (a)DSC thermograms of DGEBA-DDM-aGO at different partially cured time intervals showing the appearance of the glass transition temperature, T_g (small arrows) as well as the decrease in the heat evolution with increased time of cure (starting from top curves) (b) Comparison of reaction conversion by DSC of DGEBA-DDM (-x-), DGEBA -DDM-aGO (-•-) and DGEBA -DDM-acGO (-▲-) at different curing times, showing a lower extent of cure in the presence of aGO and a higher extent of cure in the presence acGO for the same time of cure. Dash lines represent the trendline of the individual curves.

The dynamic DSC heat flow curves of the DGEBA –DDM, DGEBA -DDM-aGO and DGEBA -DDM-acGO systems which are partially cured at different time intervals were obtained. Fig. 14(a) represents the DSC heat flow curves of DGEBA -DDM-aGO (The heat flow curves of other two systems are given in Fig 7s, supporting information). We have noticed that onset of the cure reaction (T_{onset}) increased in aGO-epoxy system (~ 108 ^{o}C) whereas it decreased slightly in acGO-epoxy system (~102 ^{o}C) compared to neat epoxy (103 ^{o}C). This indicates the acceleration effect in acGO and retardant effect by aGO on cure reaction as described at length in Section 3.2. However, ΔH_{cure} and the peak heat flow (T_p), ie., the

temperature of maximum heat flow during the cure reaction, remained largely unaffected. Significantly, we observed the heat capacity change corresponding to the appearance of T_g of the epoxy resin with the partial curing for 10-15 min or longer at 100^{o}C (arrowed in Fig. 14a). The effect of aGO and acGO on the network structure and T_g is discussed further below.

We have calculated the extent of conversion of the cure reaction (α) as a function of initial curing time using these heat flow curves and Fig. 14(b) shows the calculated data for DGEBA-DDM, DGEBA-DDM-aGO and DGEBA-DDM-acGO nanocomposites. It can be observed that values of α for DGEBA-DDM-aGO at all curing time intervals are lower than those of DGEBA-DDM. This suggests that curing reaction of epoxy was slowed down with incorporation of aGO into the epoxy matrix, consistent with the FT-IES results of Section 3.2. In contrast, addition of acGO into the epoxy matrix sped up the cure reaction producing higher values for α at the same cure time. These results further confirmed the FT-IES result that acGO can accelerate the curing reactions. Therefore, it can be seen that the presence (or absence) of OD on the GO surface greatly influences associated kinetic processes. A recent study reported the influence of OD on the kinetic process of nucleation and growth of Ag nanoparticles (AgNPs) on graphene oxide. They found that the formation of larger AgNPs on OD-free GO surface compared to smaller AgNPs on as-prepared GO. This indicates that OD plays a key role in the energetic stabilization process that allows the formation of small nanoparticles [57].

T_g and reaction conversion of epoxy and its nanocomposites at different curing time interval are shown in Table 5. In addition, T_g of cured neat resin and the composites was obtained from the 2nd heat flow curve of heat-cool-heat cycles up to 230^{o}C under same experimental conditions as in section 3.2. This is shown for DGEBA-DDM-acGO in Fig 8s, supporting Information. T_g of completely cured neat epoxy, aGO-epoxy and acGO epoxy nanocomposites were measured as ~ 94^{o}C, ~ 85^{o}C and 105^{o}C, respectively. It is clear that T_g of the aGO nanocomposite is significantly lower than that of neat epoxy matrix whereas the acGO nanocomposite has significantly higher T_g. Lower T_g is attributable to the lower cross-link density of the epoxy matrix structure in as-prepared GO nanocomposites. As discussed earlier, aGO can slow down the formation of the 3D network structure in epoxy matrix, especially near the interphase region between epoxy and aGO. This results in the presence of more linear polymer chains (Fig. 1, reaction 1) which have a higher polymer chain mobility compared to

cross-linked structures (Fig. 1, reaction 2) from reaction of the 2° amine. The higher chain mobility in the polymer matrix results in a decreased T_g of the epoxy matrix. It should be noted that as discussed above in the FT-IES study, the fraction of the resin that is in the interphase region is 30% of the total volume of resin so the effect on the lower crosslink density of the resin in this region on the overall T_g is significant. This again shows the less brittle structure of epoxy matrix in aGO nanocomposite. Furthermore, presence of OD in aGO can speed up the homopolymerization which also contribute to the formation of more linear polymer chains. On the other hand, acGO accelerates the cure, particularly the 2° amine reaction, resulting in a higher crosslink density network and consequently, more brittle structure and higher T_g.

An increase in T_g between the sample after 30 minutes reaction at 100^{o}C and after heating to 230^{o}C (Figure 8s) occurs only for acGO. From the FT-IES data for acGO there are few epoxy groups present to react and the heat evolved on further heating to 230^{o}C is only 1% of the total heat evolved (Table 5 and supporting information, Figure 7s(b)). It has been shown by Zukas [56] that DGEBA-DDM systems with amine concentrations above stoichiometry with epoxy, as in the case here, show only small further increase in T_g on heating to elevated temperatures, in contrast to systems that have a high residual epoxy content after cure. It is possible that the surface of acGO can catalyse further reaction to increase the local crosslink density and thus T_g. This reaction is not possible in the case of aGO since the catalytic sites are not accessible. Alternatively it is possible that heating above the cure temperature may achieve a more stable glassy structure for the resin and thus a higher T_g in the interphase of the acGO.

Of more significance to the mechanical properties of GO nanocomposites is the lower T_g of the interphase of aGO due to OD and the fact that heating above T_g did not change this. Therefore, we believe that in the presence of aGO, formation of three dimensional network structures in the epoxy matrix slows down, particularly near the aGO-epoxy interphase region. So the region immediately around the aGO (interphase) will have a lower crosslink density and thus a higher toughness. As a result, aGO nanocomposite shows significantly higher toughness than neat epoxy. Increase of toughness with addition of aGO into epoxy matrix has been reported in literature [15,18,58,59]. Removal of OD from aGO by autoclaving (to give acGO) reversed the overall effect of aGO by accelerating cure process, giving a more cross-linked matrix structure, lower toughness and higher T_g. The OD clearly has a major role to play in the

performance of nanocomposites by acting as a compatibilizing surfactant which is beneficial in producing nanocomposites with a good dispersion and a toughened interface between GO and a polymer matrix [60]. It is well known in carbon fibre composite technology that maximizing the reaction between the graphite surface and epoxy resin, while increasing the modulus, does not lead to the highest fracture toughness[61]. The modification of the epoxy-GO interphase by the OD to lower the crosslink density could contribute to the reported higher nanocomposite toughness. It is unlikely that the fortuitous formation of OD during preparation of GO has produced the optimum properties and this provides an area worthy of further exploration in a wider range of resins and surface treatment conditions.

Table 5

Change of T_g and reaction conversion rate at different curing time interval of DGEBA –DDM, DGEBA -DDM-aGO and DGEBA -DDM-acGO.

Time (t, min)	DGEBA-DDM		DGEBA-DDM-aGO		DGEBA-DDM-acGO	
	α	T_g (^oC)	α	T_g (^oC)	α	T_g (^oC)
0	0	-	0	-	0	-
5	0.23	-	0.17	-	0.34	-
10	0.47	-	0.39	-	0.61	45
15	0.68	51.5	0.60	42	0.79	57.5
20	0.89	73	0.80	54	0.92	73.6
25	0.94	81.3	0.92	73	0.98	87.6
30	0.98	94	0.99	84.6	0.99	91.7

4. CONCLUSIONS

We have reported a simple and quick FT-IES method to monitor the cure kinetics of epoxy curing and to evaluate the influence of aGO and removal of OD on the network formation and the rate of reaction. The technique offers an immediate assessment of the chemical changes occurring in the matrix while curing progresses. Emission spectra clearly showed the gradual decrease of peak intensities of epoxide, 1° and 2° amine bands with the time of curing as well as the increase and broadening of ether bands. This indicates the consumption of epoxide and amine

groups to form the cross-linked resin matrix. Further, the comparison studies revealed the retardant effect of aGO on the epoxy curing, principally on the reaction of the formed 2°amine with further epoxide. The retardant effect of aGO on 2° amine reactions has been linked to this oxidative debris which also enhances etherification reactions such as homopolymerization, which also lowers the crosslink density in the interphase. Removal of OD from aGO sped up the overall cure process, including 2^{o} amine reactions, so increasing the crosslink density in the epoxy matrix. It was evident that OD significantly covered the available reactive and catalytic sites in aGO surfaces and greatly influenced the catalytic behaviour of GO. FT-IES data have been confirmed by DSC studies where aGO-epoxy nanocomposite exhibited considerably lower T_g and slower reaction conversion compared to neat DGEBA-DDM resin. Removal of OD caused an increase of the cross-link density in the DGEBA-DDM matrix, consequently higher T_g and a more brittle interphase. Fig. 15 summarizes these findings.

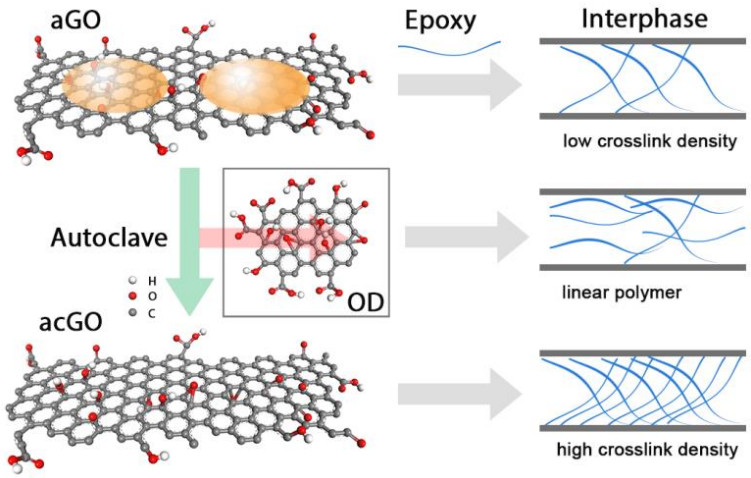

Fig. 15. Illustration of the effect of autoclave treatment to remove OD from the as-produced GO surface on the interphase structure of the cured epoxy resin due to changes in cure chemistry and crosslink density.

Therefore, it can be concluded that these chemical changes in the interphase compared to bulk are consistent with the result that low addition of aGO (commonly used as GO in polymer nanocomposites) can effectively improve the toughness of epoxy matrix. This work highlights the importance of oxidized debris in affecting the chemistry of the cure reactions leading to a novel interphase structure.

SUPPORTING INFORMATION

Preparation and characterization of GO, Isolation of oxidative debris by autoclave method, characterization and comparison of autoclaved GO with base-washed GO. This also contains further spectra and thermograms of DGEBA-DDM-aGO at 100^{o}C during cure.

ACKNOWLEDGEMENT

Authors gratefully acknowledge Dr. Barry Wood, University of Queensland, Australia for his invaluable help for XPS analysis. We are thankful to Central Analytical Research Facility at Queensland University of Technology for other characterization. We thank Queensland University of Technology for financial support.

REFERENCES

[1] Aboutalebi SH, Gudarzi MM, Zheng QB, Kim J-K.Adv. Funct. Mater. 2011;21:2978-88.

[2] Wang Y, Shi Z, Yu J, Chen L, Zhu J, Hu Z.Carbon 2012;50:5525-36.

[3] Wang X, Hu Y, Song L, Yang H, Xing W, Lu H.J. Mater. Chem. 2011;21:4222-7.

[4] Qian X, Song L, Tai Q, Hu Y, Yuen RKK.Compos. Sci. Technol. 2013;74:228-34.

[5] Liang J, Huang Y, Zhang L, Wang Y, Ma Y, Guo T, Chen Y.Adv. Funct. Mater. 2009;19:2297-302.

[6] Galpaya D, Wang M, George G, Motta N, Waclawik E, Yan C.J. Appl. Phys. 2014;116:053518-1-10.

[7] Rourke JP, Pandey PA, Moore JJ, Bates M, Kinloch IA, Young RJ, Wilson NR.Angew. Chem., Int. Ed. 2011;50:3173-7.

[8] Thomas HR, Valles C, Young RJ, Kinloch IA, Wilson NR, Rourke JP.J. Mater. Chem.C 2013;1:338-42.

[9] Bonanni A, Ambrosi A, Chua CK, Pumera M.ACS Nano 2014;8:4197-204.

[10] Ryu SH, Sin JH, Shanmugharaj AM.Eur. Polym. J. 2014;52:88-97.

[11] Gu Y, Li M, Wang J, Zhang Z.Carbon 2010;48:3229-35.

[12] McAllister MJ, Li J-L, Adamson DH, Schniepp HC, Abdala AA, Liu J, Herrera-Alonso M, Milius DL, Car R, Prud'homme RK, Aksay IA.Chem. Mater. 2007;19:4396-404.

[13] Dreyer DR, Park S, Bielawski CW, Ruoff RS.Chem. Soc. Rev. 2010;39:228-40.

[14] Paredes JI, Villar-Rodil S, Martínez-Alonso A, Tascón JMD.Langmuir 2008;24:10560-4.

[15] Bortz DR, Heras EG, Martin-Gullon I.Macromolecules 2011;45:238-45.

[16] Miller SG, Bauer JL, Maryanski MJ, Heimann PJ, Barlow JP, Gosau J-M, Allred RE.Compos. Sci. Technol. 2010;70:1120-5.

[17] Park JK and Kim DS.Polym. Eng. Sci. 2014;54:969-76.

[18] Wang X, Jin J, Song M.Carbon 2013;65:324-33.

[19] Zandiatashbar A, Picu R, Koratkar N.J. Eng. Mater. Technol. 2012;134:031011--6.

[20] Putz KW, Palmeri MJ, Cohn RB, Andrews R, Brinson LC.Macromolecules 2008;41:6752-6.

[21] Cividanes LS, Simonetti EAN, Moraes MB, Fernandes FW, Thim GP.Polym. Eng. Sci. 2013:1-11.

[22] George GA, Cash GA, Rintoul L.Polym. Int. 1996;41:169-82.

[23] St John NA and George GA.Polymer 1992;33:2679-88.

[24] Bae J, Jang J, Yoon S-H.Macromol. Chem. Phys. 2002;203:2196-204.

[25] Luo Y, Zhao Y, Cai J, Duan Y, Du S.Mater Design 2012;33:405-12.

[26] de la Vega A, Kovacs JZ, Bauhofer W, Schulte K.Compos. Sci. Technol. 2009;69:1540-6.

[27] Cividanes LS, Brunelli DD, Antunes EF, Corat EJ, Sakane KK, Thim GP.J. Appl. Polym. Sci. 2013;127:544-53.

[28] Hill DJT, George GA, Rogers DG.Polym. Adv. Technol. 2002;13:353-62.

[29] St John NA and George GA.Prog. Polym. Sci. 1994;19:755-95.

[30] Parameswaranpillai J, George A, Pionteck J, Pioneck J, Thomas S.J Polym. 2013;2013:17.

[31] Karasinski EN, Da Luz MG, Lepienski CM, Coelho LAF.Thermochim. Acta 2013;569:167-76.

[32] Hong SG and Tsai JS.J Therm Anal Calorim 2001;63:31-46.

[33] Qui SL, Wang CS, Liu CG, Chen XY, Xie HF, Huang YA, Cheng RS.eXPRESS Polym Lett 2011;5:809-18.

[34] Mauro M, Acocella MR, Corcione CE, Maffezzoli A, Guerra G.Polymer 2014;55:5612-5.

[35] Teng C-C, Ma C-CM, Lu C-H, Yang S-Y, Lee S-H, Hsiao M-C, Yen M-Y, Chiou K-C, Lee T-M.Carbon 2011;49:5107-16.

[36] Xie H, Liu B, Yuan Z, Shen J, Cheng R.J. Polym. Sci., Part B: Polym. Phys. 2004;42:3701-12.

[37] Valentini L, Armentano I, Puglia D, Kenny JM.Carbon 2004;42:323-9.

[38] Kim J-i, Kang PH, Nho YC.J. Appl. Polym. Sci. 2004;92:394-401.

[39] Hardis R, Jessop JLP, Peters FE, Kessler MR.Composites Part A 2013;49:100-8.

[40] Marcano DC, Kosynkin DV, Berlin JM, Sinitskii A, Sun Z, Slesarev A, Alemany LB, Lu W, Tour JM.ACS Nano 2010;4:4806-14.

[41] Montes-Navajas P, Asenjo NG, Santamaría R, Menéndez R, Corma A, García H.Langmuir 2013;29:13443-8.

[42] Park JK and Kim DS.Polym. Eng. Sci. 2013:1-8.

[43] Vassallo AM, Cole-Clarke PA, Pang LSK, Palmisano AJ.Appl. Spectrosc. 1992;46:73-8.

[44] Bao C, Guo Y, Song L, Kan Y, Qian X, Hu Y.J. Mater. Chem. 2011;21:13290-8.

[45] Sun L, Wang L, Tian C, Tan T, Xie Y, Shi K, Li M, Fu H.RSC Advances 2012;2:4498-506.

[46] Mou Z, Chen X, Du Y, Wang X, Yang P, Wang S.Appl. Surf. Sci. 2011;258:1704-10.

[47] Su C, Acik M, Takai K, Lu J, Hao S-j, Zheng Y, Wu P, Bao Q, Enoki T, Chabal YJ, Ping Loh K.Nat Commun 2012;3:1298.

[48] Tang T, Liu F, Liu Y, Li X, Xu Q, Feng Q, Tang N, Du Y.Appl. Phys. Lett. 2014;104:123104.

[49] López-Díaz D, Mercedes Velázquez M, Blanco de La Torre S, Pérez-Pisonero A, Trujillano R, Fierro JLG, Claramunt S, Cirera A.ChemPhysChem 2013;14:4002-9.

[50] Zhou Y, Bao Q, Tang LAL, Zhong Y, Loh KP.Chem. Mater. 2009;21:2950-6.

[51] Stankovich S, Dikin DA, Piner RD, Kohlhaas KA, Kleinhammes A, Jia Y, Wu Y, Nguyen ST, Ruoff RS.Carbon 2007;45:1558-65.

[52] Mijović J and Andjelić S.Polymer 1996;37:1295-303.

[53] St John NA.PhD Thesis 1993;University of Queensland, Australia.

[54] Verma S, Mungse HP, Kumar N, Choudhary S, Jain SL, Sain B, Khatri OP.Chem. Commun. (Cambridge, U. K.) 2011;47:12673-5.

[55] Dreyer DR, Jarvis KA, Ferreira PJ, Bielawski CW.Macromolecules 2011;44:7659-67.

[56] Zukas WX.J. Appl. Polym. Sci. 1994;53:429-40.

[57] Faria AF, Martinez DST, Moraes ACM, Maia da Costa MEH, Barros EB, Souza Filho AG, Paula AJ, Alves OL.Chem. Mater. 2012;24:4080-7.

[58] Yang H, Shan C, Li F, Zhang Q, Han D, Niu L.J. Mater. Chem. 2009;19:8856-60.

[59] Tang L-C, Wan Y-J, Yan D, Pei Y-B, Zhao L, Li Y-B, Wu L-B, Jiang J-X, Lai G-Q.Carbon 2013;60:16-27.

[60] Vallés C, Kinloch IA, Young RJ, Wilson NR, Rourke JP.Compos. Sci. Technol. 2013;88:158-64.

[61] Downing TD, Kumar R, Cross WM, Kjerengtroen L, Kellar JJ.Journal of Adhesion Science and Technology 2000;14:1801-12.

Supporting information

Preparation of GO

GO was prepared by oxidation of graphite flakes according to the modified Hummers method [1]. In brief, a mixture of graphite and $KMnO_4$ (Ratio of 1:6) was added into a beaker containing mixture of H_2SO_4:H_3PO_4 (9:1) acids. Then the reaction mixture was stirred while heating at 50^oC for 12 h. The reaction mixture was cooled down to room temperature and poured onto ice cubes with 3 ml of 30% H_2O_2. Then the mixture was sieved through a metal US standard testing sieve (250 μm). The filtrate was centrifuged at 4000 rpm for 30 minutes. The precipitate was washed with DI water, HCl and ethanol. For each wash, the mixture was sieved through US standard testing sieve followed by centrifuging at 4000 rpm for 30 min. The final precipitate was dissolved in DI water and sonicated for 1 h. Finally, the GO aqueous dispersion was freeze for 24h followed by freeze drying at -51^oC under vacuum condition for 72 h. The final product is called as aGO.

Preparation of acGO and isolation of OD

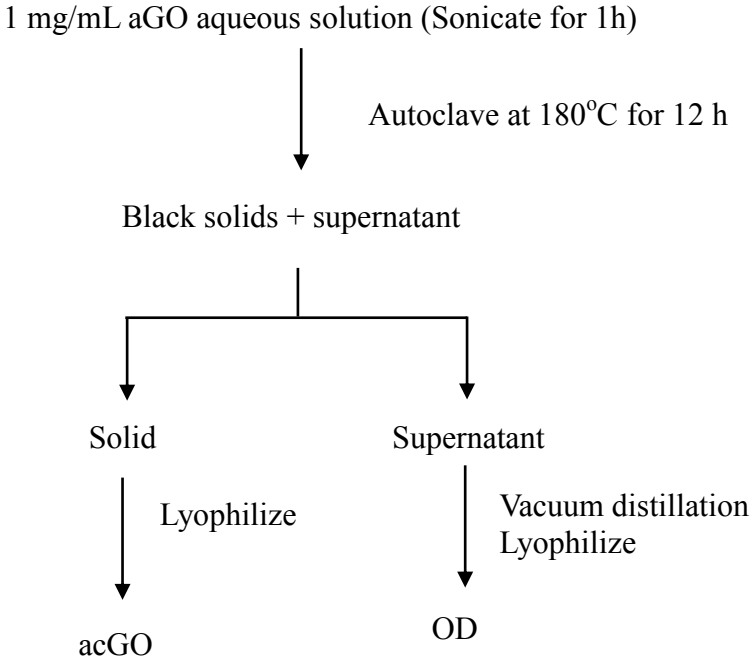

Scheme 1s. Preparation of acGO and recovery of OD from aGO

Autoclaved GO(acGO) was prepared from aGO and separated from the Oxidative Debris (OD) as shown in Fig. 1s and were collected and named as Oxidative debris (OD). We produced base washed GO (bwGO) following the procedure reported elsewhere [2-5] to compare with acGO.

Characterization of aGO and acGO

X-ray diffraction (XRD) powder patterns were taken on a conventional X-ray diffractometer (XRD, PANalytical Cu MPD) using Cu kα radiation. Raman spectra of samples were recorded from 1250 to 3000 cm^{-1} on a Renishaw inVia Raman Microscope using a 532 nm edge filter laser beam. IR spectra were obtained using FTIR 5700 Nicolet Diamond ATR spectrometer. The spectrum resolution was 4 cm^{-1} in the range from 800 to 4000 cm^{-1}. 64 scans were performed to get the average spectrum. The microstructural characterizations were performed using a JEOL-7001F field-emission scanning electron microscope (FESEM) operated at 15 kV and a JEOL 1400 transmission emission microscope (TEM) operated at 120 kV. Dry aGO powder was used for the FESEM analysis. Clear solution of aGO in DMF was dropped cast onto carbon coated copper TEM grid for TEM analysis. Samples for atomic force microscope (AFM) imaging were prepared by depositing clear solution of aGO (in DMF) on freshly cleaved mica surface. AFM images were taken using a BMT multi-scan AFM with silicon tip. Tapping mode was applied to get the topography of the GO flakes at the scan rate of 1.2 Hz with surface area of 5 x 5μm^2.

Surface area of aGO was measured, by the Methylene Blue (MB) method reported by Navajas et al.[6] starting from an aqueous dispersion of a known weight of aGO to which increasing amounts of MB were added, following the evolution of the visible transmittance spectra. Concentrations of aGO dispersions were 0.043 and 0.085 μg/μl and concentration of stock aqueous solution of MB was 0.3 μg/μl. Transmittance spectra were recorded by placing 2 ml of aGO aqueous solution in 1cm path length quartz cuvette and adding small aliquots (5 μl initially and 1 μl near end point) of MB stock aqueous solution of 0.3 μg/μl under continuous magnetic stirring, using an Ocean USB4000 Fibre Optics spectrometer. The baselines of the spectra were corrected by subtracting the initial aGO transmittance and then transmittance spectra were converted to absorbance. The addition of MB was continued up to blue

precipitation. The value of the amount of MB corresponding to the maximum intensity of the 580 nm band was taken as indicative of complete surface coverage of aGO [6].

Results

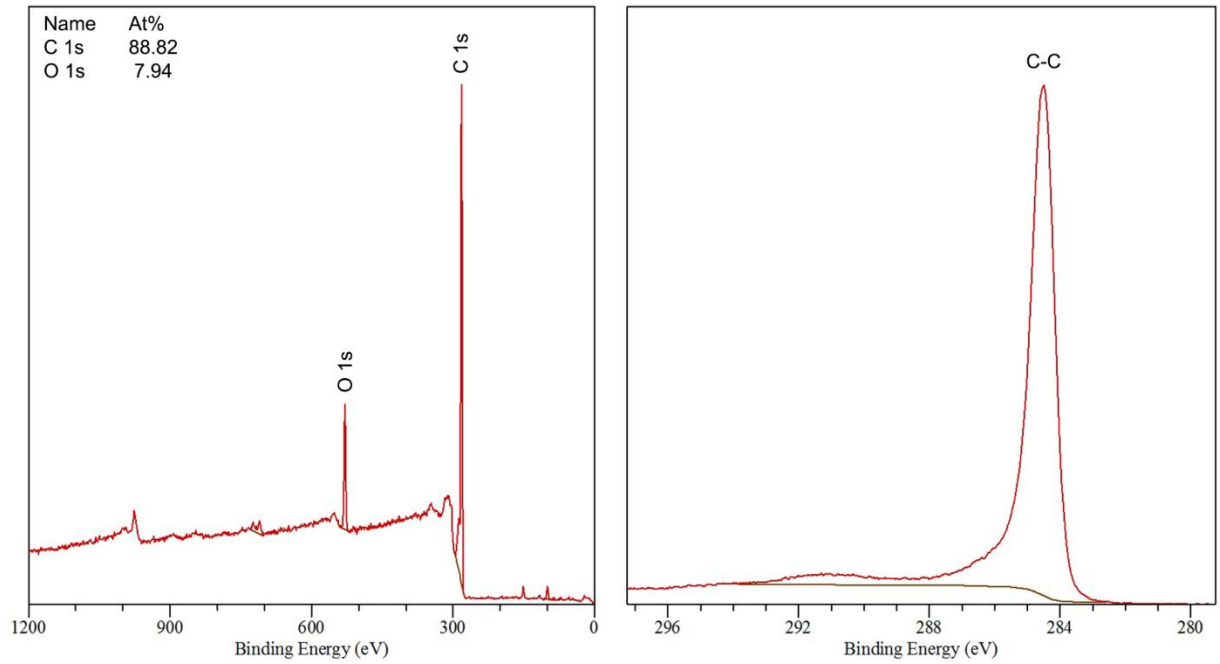

Figure 2s. XPS survey spectrum and C 1s XPS multiplex spectrum of graphite

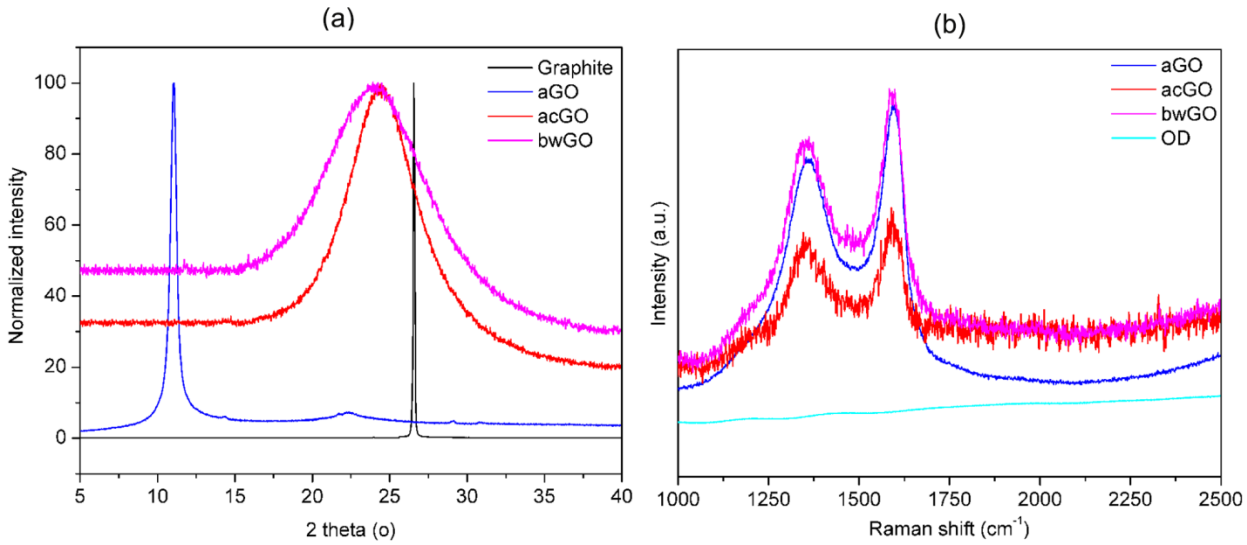

Figure 2s. (a) XRD of aGO, acGO and bwGO (b) Raman of aGO, acGO, bwGO and OD

To analyse the effect of purification processes on the interlayer structure, we obtained the XRD pattern of the samples, Fig. 2s (a). aGO diffractogram presents a peak around 11°. This

peak is characteristic of 002 plane of graphite compounds and the interlayer distance calculated is ~0.93 nm. This value is similar to graphene oxide reported in literature [7,8]. The purification process leads to a shift towards higher angle value of the (002) diffraction peak. The interlayer distance values for acGO and bwGO were 0.36 and 0.37 nm, respectively indicating that the purification process decreases the interlayer distance. This could be due to the elimination of the OD located at the interlayer [9]. It also confirmed that both purification processes resulted in a product that is structurally similar.

The spectra in Fig. 2s (b) show the two characteristic raman bands of graphene derivatives, centred at 1597 cm^{-1} (G band) and 1350 cm^{-1} (D band) respectively. The value of I_D/I_G ratio was almost identical for all three samples, ie. aGO, acGO and bwGO (~0.77) suggesting that the graphene sheets are not altered themselves by purification [2,9]. The raman spectra of OD does not show any evidence of G or D bands [3] consistent with it not being graphene-like.

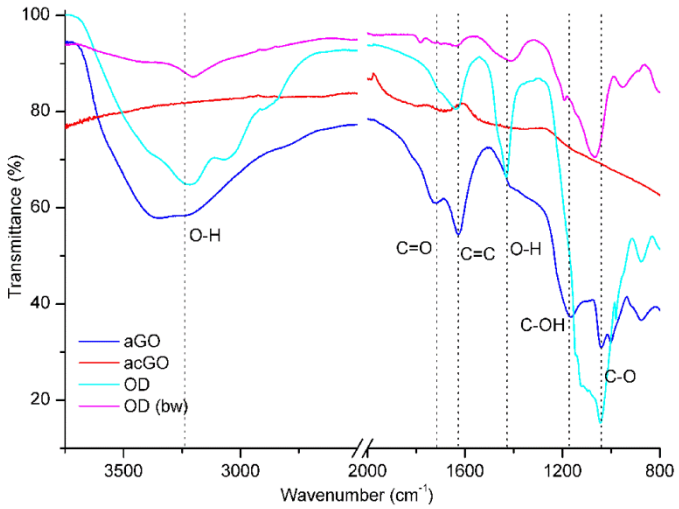

Figure 3s. FTIR of aGO, acGO and OD

As shown in Fig 3s, the FTIR transmittance spectrum of aGO shows a broad peak at 3800-2500 cm^{-1} (OH and H_2O) and several peaks between 1800 and 800 cm^{-1}. These peaks can be assigned to carboxyl, ketone, hydroxyl, epoxide and C=C bonding as labelled in the figure [2,3,9,10]. The FTIR spectra of both ODs (from autoclaved and base washed) are similar to that of aGO, even as the spectrum of acGO is comparatively featureless. Therefore, we conclude that

OD is heavily oxidized with similar functionalized groups to aGO and degree of functionalization is decreased with purification processes.

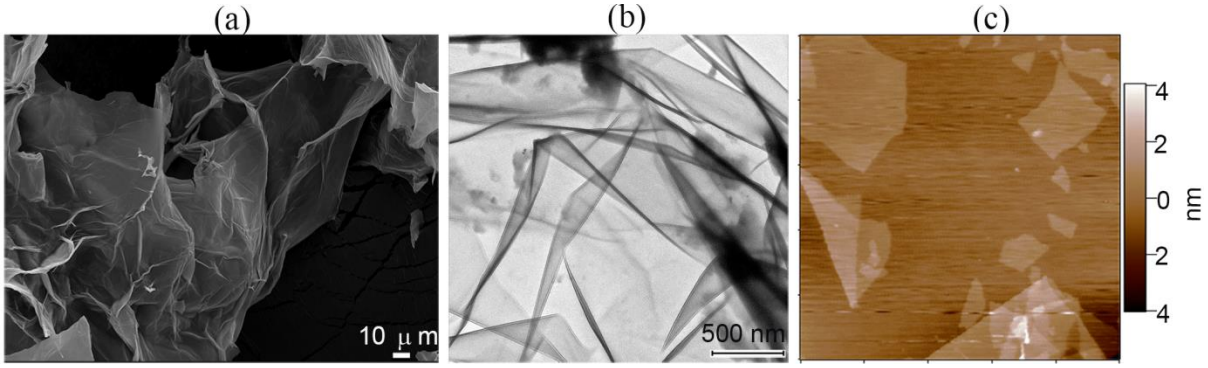

Figure 4s. (a) SEM (b) TEM (c) AFM images of aGO

Fig. 4s illustrates typical SEM, TEM and AFM micrographs of aGO [1,11]. Generally, morphology of graphene sheets is not affected by purification process. But there should be some changes in layer thickness of the sheets in purified GO which would be able to be observed by AFM topography [4].

Surface area measurements of aGO

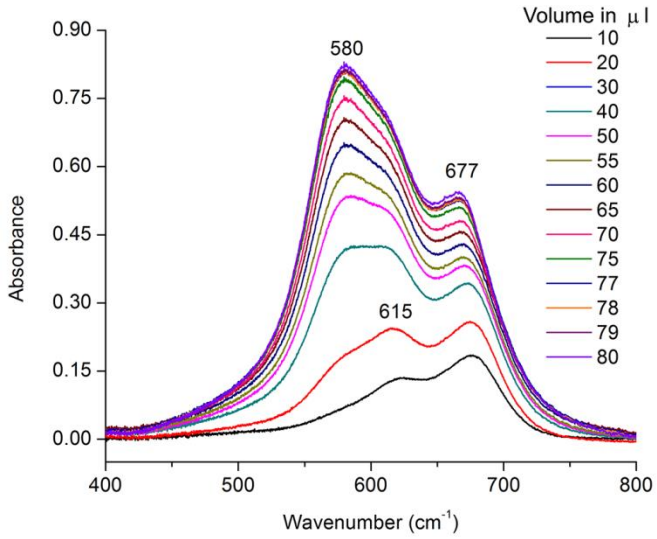

Figure 5s. Visible absorption spectra of aqueous dispersion of aGO (a) 0.043 μg/μl upon addition of increasing volume of a MB stock solution (0.3 μg/μl). The baseline of the spectra has been corrected subtracting the initial aGO absorption.

Surface area of GO was calculated using the changes in UV Visible absorption spectra of an aqueous aGO solution upon the addition of MB. We observed identical spectra and spectral changes with MB addition as reported by Navajas et al.[6] At low MB concentration, two peaks were observed at 667 nm and 615 nm which are attributed to aGO and MB π clouds overlapping and interactions between MB molecules adsorbed on aGO. With increasing MB concentration a new peak appeared at 580 nm, which is attributed to close packing of MB on upper and lower surfaces of aGO. Further addition of MB, increased the intensity of latter peak and the maximum intensity was observed just before the formation of a blue colour precipitate suggesting complete surface coverage of aGO by MB adsorption (Figure 5s). The amount of MB used up at maximum intensity is 79 µl and the estimated surface area of aGO is 719 m^2/g considering 2.54 m^2 as the area covered by 1 mg of MB [6,12]. Calculated surface area of aGO is comparable to values reported in literature [6,12].

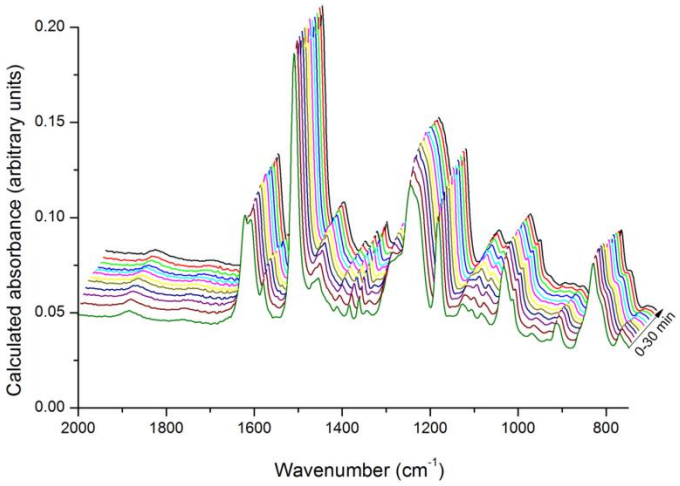

Figure 6s. Stack plot of successive spectra of DGEBA-DDM-aGO at 100 ^oC for cure up to 30 minutes.

Fig. 6s illustrates the spectra of DGEBA-DDM-aGO at 100 ^oC for cure up to 30 minutes. Similar spectra were observed for DGEBA-DDM-acGO and DGEBA-DDM-OD.

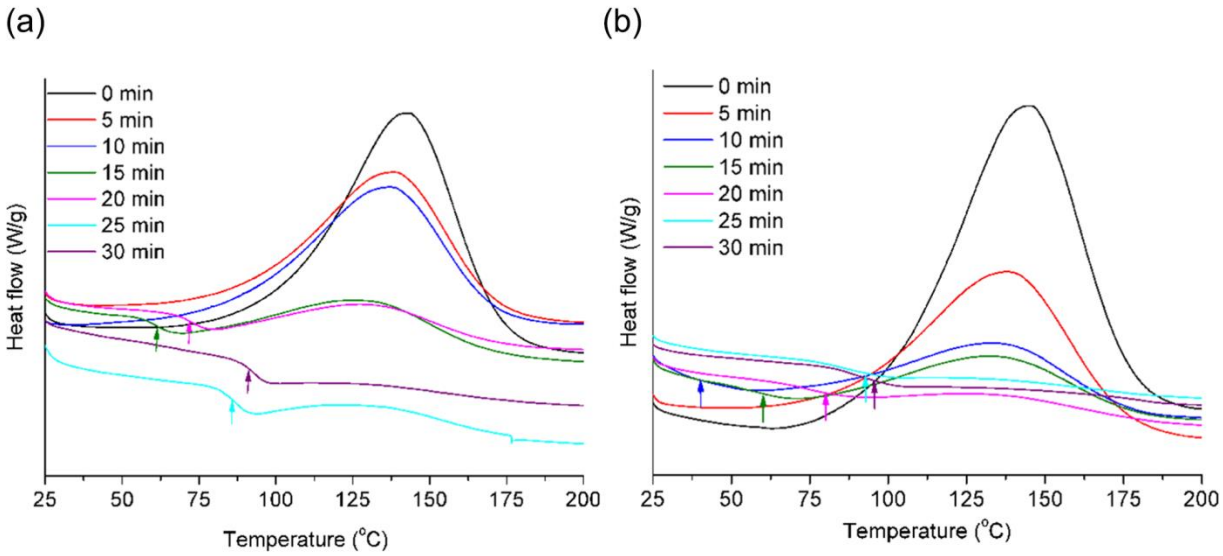

Fig. 7s. DSC thermograms of (a) DGEBA-DDM (b) DGEBA-DDM-acGO at different partially cured time intervals showing the appearance of the glass transition temperature, T_g (small arrows) as well as the decrease in the heat evolution with increased time of cure (starting from top curves).

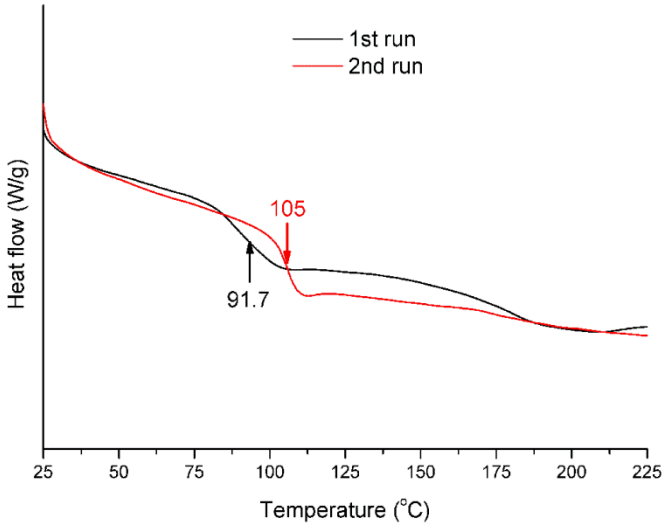

Fig. 8s. DSC thermograms of DGEBA-DDM-acGO partially cured at 100°C for 30 min showing the initial T_g of 91.7°C and the second run after the sample was heated to 230°C at 10°C/min and cooled to 25°C before reheating. It is seen that T_g then increased to 105°C. Neither DGEBA-DDM nor DGEBA-DDM-aGO showed any increase in T_g after heating to 230°C.

References

[1] Marcano DC, Kosynkin DV, Berlin JM, Sinitskii A, Sun Z, Slesarev A, Alemany LB, Lu W, Tour JM.ACS Nano 2010;4:4806-14.

[2] Rourke JP, Pandey PA, Moore JJ, Bates M, Kinloch IA, Young RJ, Wilson NR.Angew. Chem., Int. Ed. 2011;50:3173-7.

[3] Guo Z, Wang S, Wang G, Niu Z, Yang J, Wu W.Carbon 2014;76:203-11.

[4] Faria AF, Martinez DST, Moraes ACM, Maia da Costa MEH, Barros EB, Souza Filho AG, Paula AJ, Alves OL.Chem. Mater. 2012;24:4080-7.

[5] Coluci VR, Martinez DST, Honório JG, de Faria AF, Morales DA, Skaf MS, Alves OL, Umbuzeiro GA.J. Phys. Chem. C 2014;118:2187-93.

[6] Montes-Navajas P, Asenjo NG, Santamaría R, Menéndez R, Corma A, García H.Langmuir 2013;29:13443-8.

[7] Compton OC, Jain B, Dikin DA, Abouimrane A, Amine K, Nguyen ST.ACS Nano 2011;5:4380-91.

[8] Liu F, Song S, Xue D, Zhang H.Adv. Mater. 2012;24:1089-94.

[9] López-Díaz D, Mercedes Velázquez M, Blanco de La Torre S, Pérez-Pisonero A, Trujillano R, Fierro JLG, Claramunt S, Cirera A.ChemPhysChem 2013;14:4002-9.

[10] Tang T, Liu F, Liu Y, Li X, Xu Q, Feng Q, Tang N, Du Y.Appl. Phys. Lett. 2014;104:123104.

[11] Galpaya D, Wang M, George G, Motta N, Waclawik E, Yan C.J. Appl. Phys. 2014;116:053518-1-10.

[12] McAllister MJ, Li J-L, Adamson DH, Schniepp HC, Abdala AA, Liu J, Herrera-Alonso M, Milius DL, Car R, Prud'homme RK, Aksay IA.Chem. Mater. 2007;19:4396-404.